JCI The Journal of Clinical Investigation

Macrophage monocarboxylate transporter 1 promotes peripheral nerve regeneration after injury in mice

Mithilesh Kumar Jha, … , Jeffrey D. Rothstein, Brett M. Morrison

J Clin Invest. 2021. https://doi.org/10.1172/JCI141964.

Research In-Press Preview Metabolism Neuroscience

Graphical abstract

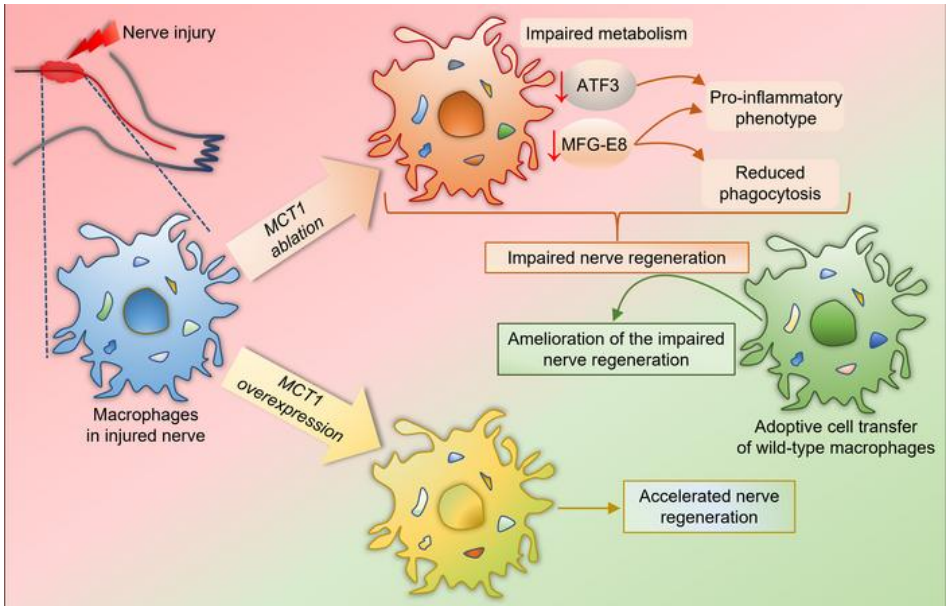

Macrophage monocarboxylate transporter 1 promotes peripheral nerve regeneration after injury in mice

Mithilesh Kumar Jha[1], Joseph V. Passero[1], Atul Rawat[1], Xanthe Heifetz Ament[1], Fang Yang[1], SvetlanaVidensky[1], Samuel L. Collins[2], Maureen R. Horton[2], Ahmet Hoke[1], Guy A. Rutter[3], Alban Latremoliere[4], Jeffrey D. Rothstein[1], Brett M. Morrison[1,*]

[1]Department of Neurology, Johns Hopkins University School of Medicine, Baltimore, Maryland, USA
[2]Department of Medicine, Johns Hopkins University School of Medicine, Baltimore, Maryland, USA
[3]Section of Cell Biology and Functional Genomics, Division of Diabetes, Endocrinology and Metabolism, Department of Metabolism, Digestion and Reproduction, Imperial College London, London, UK
[4]Department of Neurosurgery, Johns Hopkins University School of Medicine, Baltimore, Maryland, USA

The authors have declared that no conflict of interest exists.

*To whom correspondence should be addressed:
Brett M. Morrison M.D., Ph.D.
855 North Wolfe Street, Rangos 248, Baltimore, MD 21205, USA
E-mail: bmorris7@jhmi.edu, Phone: 410-502-0796, Fax: 410-502-5459

Conflict of Interest: The authors have declared that no conflict of interest exists.

Abstract

Peripheral nerves have the capacity for regeneration, but the rate of regeneration is so slow that many nerve injuries lead to incomplete recovery and permanent disability for patients. Macrophages play a critical role in the peripheral nerve response to injury, both for Wallerian degeneration and for contributing to regeneration, and their function has recently been shown to be dependent on intracellular metabolism. To date, the impact of their intracellular metabolism on peripheral nerve regeneration has not been studied. Examining conditional transgenic mice with selective ablation of solute carrier family 16, member 1 (*Slc16a1*, which encodes the monocarboxylate transporter 1, MCT1) in macrophages, we found that MCT1 contributes to macrophage metabolism, phenotype, and function, specifically in regard to phagocytosis and supporting peripheral nerve regeneration. Adoptive cell transfer of wild-type macrophages ameliorated the impaired nerve regeneration in macrophage-selective MCT1 null mice. We also developed a mouse model that overexpresses MCT1 in macrophages and found that peripheral nerves in these mice regenerated more rapidly than control mice. Our study provides further evidence that MCT1 has an important biological role in macrophages and that manipulations of macrophage metabolism can enhance recovery from peripheral nerve injuries, for which there are currently no approved medical therapies.

Introduction

Recovery from peripheral nerve injury, which can occur from trauma, surgical iatrogenesis, medications, or toxins, depends on a carefully orchestrated series of events within injured axons and non-neuronal cells, particularly Schwann cells (SCs) and macrophages (1, 2). In the peripheral nerve distal to the site of injury, SCs release their myelin, de-differentiate, proliferate, and secrete factors to recruit inflammatory cells (3). Axons subsequently degenerate due to multiple factors, including energy failure and reduced neurotrophic support (4-6), and circulating neutrophils and macrophages are recruited, along with resident macrophages, to phagocytose axonal and myelin debris, which assists axonal regeneration and remyelination (7). Though the peripheral nervous system is capable of regenerating following injury, the speed of regeneration is quite slow with a rate of approximately 1 mm/day in humans and 3-5 mm/day in rodents (8-11). Given that human peripheral nerves are up to 1 meter long, some nerve injuries require regeneration over long distances and incomplete recovery occurs due to the loss of regeneration-promoting signals prior to the nerve reaching its destination (6). Emerging evidence shows that infiltrating and resident macrophages are critical contributors to axonal regeneration by removing inhibitory myelin and axonal debris, adopting a pro-regenerative phenotype, secreting cytokines and growth factors that impact SC function and nerve regeneration, and potentially providing metabolic support to axons (12). Although the contribution of macrophages to clearance of myelin debris in Wallerian degeneration has been universally acknowledged and accepted (13), their role in positively influencing the regeneration processes has been recognized only more recently (12, 14-17).

Macrophages are abundant not only during nerve degeneration, but also while the nerves

are regenerating (7). Macrophages secrete cytokines that trigger growth factor synthesis in non-neuronal cells in the nerve and produce factors that facilitate SC migration and axon regeneration (7, 18). The capacity of macrophages to adopt pro-inflammatory or anti-inflammatory or pro-regenerative states creates a favorable microenvironment for both the initial rapid infiltration of the nerve, where pro-inflammatory macrophages predominate, and the subsequent Wallerian degeneration, nerve regeneration and remyelination, when pro-regenerative macrophages predominate (12, 19-23). The capacity of macrophages to respond to external stimuli is not uniform, rather it is modulated by cross-talk between intracellular signaling cascades and metabolic pathways (24-28), and these pathways govern macrophage phenotype at least partly by altering gene expression that directly modifies cellular metabolism (29-31). Besides intracellular metabolic adaptation, macrophages can also impact metabolism in surrounding SCs and neurons following nerve injury by secreting factors (32). Though only recently explored for their role in immune biology, monocarboxylate transporters (MCTs), particularly MCT1 (encoded by solute carrier family 16, member 1, *Slc16a1*), are proving to be critical for regulating diverse immune cell functions (33-37). The role of MCT1 in macrophage immune and metabolic functions and their contributions to nerve injury and regeneration biology has not previously been defined.

Here, using macrophage-selective MCT1 ablation or upregulation mice and adoptive cell transfer of macrophages, we identified a crucial role for MCT1 in determining macrophage intracellular metabolism and immune functions in the peripheral nerve response to injury. We found that macrophage-specific MCT1 deletion impairs axon regeneration by reducing the phagocytic capacity of macrophages and inhibiting the formation of pro-regenerative microenvironment in injured nerves, which is potentially being regulated by activating transcription factor 3 (ATF3). Importantly, the adoptive cell transfer of macrophages with intact

MCT1 was able to completely ameliorate the impaired peripheral nerve regeneration in mice with macrophage-selective ablation of MCT1. Of particular clinical interest, we observed that MCT1 upregulation in macrophages accelerates peripheral nerve regeneration following injury, which may be a promising pathway for treating peripheral nerve injuries, a common clinical problem worldwide with no therapeutic options.

Results

Macrophage-selective MCT1 ablation impairs peripheral nerve regeneration

In a prior publication from our laboratory, we demonstrated that transgenic mice with partial MCT1 deficiency in all cells (MCT1 heterozygous null mice) have impaired nerve regeneration after injury (38). MCT1 is expressed in virtually all cells (39); and thus, this initial paper provided no further understanding of the cell-specific function of MCT1 in the cascade of cellular and molecular events following peripheral nerve injury. In order to dissect the specific role for MCT1 in peripheral nerve regeneration and identify its translational significance, MCT1 was selectively ablated from macrophages, perineurial cells, Schwann cells, and DRG neurons, all of which participate in nerve regeneration and express MCT1, by mating our conditional MCT1 null mouse ($MCT1^{f/f}$) with 4 different cell-specific cre mouse lines (Figures 1A and 2). With the exception of the Schwann cell-specific deletion of MCT1, which was validated and published recently (40), the other mice were validated prior to being evaluated for nerve regeneration (Figure 3 and Supplemental Figures 1 and 2). Peritoneal exudative macrophages isolated from mice with macrophage-specific MCT1 deficiency (LysM-Cre:$MCT^{f/f}$) have both reduced expression of MCT1 (Figure 3A) and lactate transport (Figure 3B). They have a compensatory increase in MCT2 and GluT3, but not MCT4 or GluT1 (Figure 3, C to F).

Following sciatic nerve crush in proximal thigh (Figure 1B), there was a delay in nerve regeneration, measured electrophysiologically by slowed recovery of motor nerve condition velocity (NCV; Figure 1C) and compound muscle action potentials (CMAPs; Figure 1D) in male LysM-Cre:MCT$^{f/f}$ mice. Slow electrophysiological recovery after nerve injury was also confirmed in female mice, suggesting that the delayed regeneration after nerve injury observed due to MCT1 deficiency in macrophages is independent of gender (Supplemental Figure 3). The degree of motor and sensory recovery was further measured by evaluating NMJ distribution in gastrocnemius muscle and morphometric analysis of sural nerves, respectively. At 6 weeks after nerve crush, NMJ full reinnervation was significantly less in LysM-Cre:MCT$^{f/f}$ mice (Figure 1, E to H). Myelin was thinner (reflected by increased *g* ratio) at 3 and 6 weeks (Figure 1, I to K and N to P, respectively) and the number of regenerated myelinated axons was reduced at 3 weeks (Figure 1M) after sciatic nerve crush in LysM-Cre:MCT$^{f/f}$ mice. In contrast, the axon counts in sural nerves for regenerated myelinated (Figure 1R) and regenerated unmyelinated (quantified from electron micrographs, Supplemental Figure 4) at 6 weeks after sciatic nerve crush in LysM-Cre:MCT$^{f/f}$ mice were unchanged from their littermate controls. We were unable to count the number of regenerated unmyelinated axons in sural nerves 3 weeks after sciatic nerve crush as it was not possible to definitively differentiate regenerating unmyelinated axons from the degenerating axons and non-axonal structures in electron micrographs. The axonal counts confirm a role for macrophage MCT1 in regeneration of myelinated axons, but whether there is a similar role in regeneration of unmyelinated axons remains unclear. Besides highlighting the importance of macrophage intracellular metabolism in nerve regeneration, the thinner myelin and the lower number of regenerated axons in mice having MCT1-deficient macrophages could also indicate that lactate released by macrophages could be used by Schwann cells to produce myelin

and to support regenerating axons after injury. Despite delaying axonal regeneration, remyelination, nerve conduction, and NMJ reinnervation, macrophage-specific MCT1 deficiency did not impact the motor (Supplemental Figure 5, A and B) or sensory (Supplemental Figure 5, C and D) functional recovery following sciatic nerve injury. For all other cell types, the conditional deletion of MCT1 had no impact on nerve regeneration, as measured electrophysiologically, following sciatic nerve crush (Figure 2). From these studies, we conclude that MCT1 expressed in macrophages, but not in perineurial cells, Schwann cells, or DRG neurons, plays a role in peripheral nerve regeneration and its deficiency impairs peripheral nerve recovery following injury.

Macrophage MCT1 modulates inflammatory cytokine expression in injured peripheral nerves without impairing macrophage recruitment

Neuroimmune interactions play a crucial role in peripheral nerve regeneration after injury. Pro-regenerative macrophages are active participants in tissue repair and remodeling, and several recent studies acknowledge their crucial role in peripheral nerve regeneration after injury as well (14). Nerve injury disrupts the axon/Schwann cell nerve unit, which results in production of chemokines and cytokines to activate resident nerve macrophages and recruit circulating monocytes/macrophages (41-43). Recruited macrophages are crucial to remove debris (Wallerian degeneration) and promote regeneration. Removing MCT1 from macrophages in LysM-Cre:MCT$^{f/f}$ mice neither delayed nor reduced their recruitment to the nerve distal to the site of injury (Figure 4 A, B), as measured by the Iba1-positive macrophage counts in the injured nerves at 3 days (left panel) and 7 days (right panel) post-injury, suggesting that macrophage recruitment itself is unaffected due to MCT1 deficiency. In addition to expressing highly and

recombining in macrophages (44-46), LysM-Cre is also expressed in granulocytes (46, 47), especially neutrophils (44). Since neutrophils also express MCT1 (48) and have recently been shown to play a role in Wallerian degeneration following nerve injury (49), we also evaluated whether neutrophil migration following nerve injury was altered in LysM-Cre:MCT1$^{f/f}$ mice. Neutrophils are recruited to the endoneurium immediately after injury and persist for 2-3 days, where they are important for cytokine generation and modulating macrophage phenotype and function (49-51). Ly6G is expressed most highly in murine neutrophils (52). We detected Ly6G mRNA and protein expression following nerve crush. Ly6G immunofluorescence in wild-type mice was detected at 1 and 2 days, but not 3 days, following sciatic nerve crush (Supplemental Figure 6). It is not clear why we were unable to detect Ly6G immunofluorescence in 3 day crushed nerves, as reported previously (49), but this likely represents technical differences. Importantly, there was no change in Ly6G mRNA expression in injured nerves at 1 day following injury between LysM-Cre:MCT$^{f/f}$ and MCT$^{f/f}$ mice (Figure 4C), suggesting no discrepancy in neutrophil infiltration to the site of injury following MCT1 deletion.

In order to assess for alterations in macrophage or neutrophil phenotype, we quantified select pro-inflammatory and pro-regenerative cytokines from sciatic nerve at 1, 3, and 10 days following crush (Figure 4, D to I). These specific time points were chosen because 1 day represents activation of neutrophils and nerve resident macrophages, 3 days is the time for maximal pro-inflammatory cytokines from circulating macrophages, and 10 days is the stage of maximal pre-regenerative cytokines from circulating macrophages (7). As expected, uncrushed nerves had minimal expression of cytokines at any time point and there was no difference between LysM-Cre:MCT$^{f/f}$ and MCT$^{f/f}$ mice. At 1 day following crush, two prototypic pro-inflammatory cytokines that have been implicated as main effectors in diverse inflammatory

cascades, interleukin-1β (IL-1β) and tumor necrosis factor-α (TNF-α), were significantly increased in LysM-Cre:MCT$^{f/f}$ mice (Figure 4, D and E). At 3 days after crush, IL-1β was increased, though this change was not statistically significant (Figure 4F), while TNF-α was not changed in LysM-Cre:MCT$^{f/f}$ mice (Supplemental Figure 7A). By 10-day post-crush, IL-1β was not different between LysM-Cre:MCT$^{f/f}$ and MCT$^{f/f}$ mice (Supplemental Figure 7C). For the assessment of pro-regenerative macrophages, we measured the expression of chitinase-like 3 (Ym-1) and arginase, type I (Arg-1), which are markers for murine, but not human, alternatively activate myeloid cells (53). In contrast to the overall increased expression of pro-inflammatory cytokines, these pro-regenerative cytokines were generally reduced in LysM-Cre:MCT$^{f/f}$ mice. Ym-1 was reduced in the sciatic nerve of LysM-Cre:MCT$^{f/f}$ mice at 3 and 10 days and Arg-1 at 10 days following crush (Figure 4, G to I and Supplemental Figure 7B). Many of these cytokines that are altered in mice with macrophage-specific ablation of MCT1 are not only produced by macrophages. Besides infiltrated hematogenous and resident endoneurial macrophages (14, 54, 55), most of these cytokines are also expressed by infiltrated neutrophils (56) and Schwann cells (57-59) in peripheral nerves. The alterations in neutrophil gene expression may be directly from MCT1 ablation, since LysM also recombines in neutrophils. As for Schwann cells, any impact on these cells is likely downstream from MCT1 deficiency in macrophages and neutrophils. Taken together, these findings suggest that MCT1 contributes to macrophage phenotype and the cytokine microenvironment of injured nerves.

MCT1 contributes to metabolic function of macrophages *in vitro*

In recent years, intracellular metabolism has been acknowledged as a key determinant of macrophage phenotype and function (28). To understand the metabolic impact of MCT1

deletion, we measured the capacity for glycolysis and oxidative metabolism of macrophages with and without MCT1 by quantifying the rate of extracellular cellular acidification rate (ECAR; Figure 5A) and real-time oxygen consumption (OCR; Figure 5B), respectively, in a live cell assay with the Seahorse extracellular flux analyzer. Macrophages derived from LysM-Cre:MCT$^{f/f}$ mice have significantly reduced ECAR during basal respiration as well as oligomycin-induced ECAR, an indicator of glycolytic activity (Figure 5C). Similarly, basal oxygen consumption and uncoupled respiration (the maximal mitochondrial oxygen consumption capacity following the addition of FCCP), which mimics a physiologic "energy demand," was significantly decreased in macrophages isolated from LysM-Cre:MCT$^{f/f}$ mice (Figure 5, A and D). Importantly, macrophages from LysM-Cre:MCT$^{f/f}$ mice have significantly reduced spared respiratory capacity (SRC) (Figure 5E), which is defined as the difference between maximal and basal respiration, indicating reduced capacity to respond properly to increased energy demand. As would be expected, the overall ATP production for macrophages isolated from LysM-Cre:MCT$^{f/f}$ mice was reduced (Figure 5F). Interestingly, the percentage of ATP produced from glycolysis (55.8% MCT$^{f/f}$ versus 62.4% for LysM-Cre:MCT$^{f/f}$) and oxidative metabolism (44.2% MCT$^{f/f}$ versus 37.6% for LysM-Cre:MCT$^{f/f}$) was unaltered (2-way ANOVA, genotype factor ns). These findings demonstrate that MCT1 ablation in macrophages impairs both glycolytic and mitochondrial functions, reduces ATP production, and worsens metabolic adaptability to tackle stress stimuli and/or high metabolic demands.

MCT1 regulates macrophage phenotype and is critical for phagocytosis

The impaired intracellular metabolism and worsened metabolic adaptability of macrophages due to MCT1 ablation led us to investigate the role of MCT1 in determining

macrophage phenotypes and capacity for phagocytosis. Reducing MCT1 likely contributes to the induction of the pro-inflammatory phenotype since macrophages isolated from control mice exposed to pro-inflammatory phenotype inducer for 3 hours had significantly reduced expression of MCT1 (Supplemental Figure 8A), while exposure to pro-regenerative phenotype inducer led to an insignificant trend toward increased MCT1 expression (Supplemental Figure 8B). The importance of MCT1 for determining macrophage phenotype was confirmed in periteoneal exudative macrophages prepared from LysM-Cre:$MCT^{f/f}$ and $MCT^{f/f}$ mice. These macrophages were challenged with either LPS plus IFN-γ or IL-4, well-known inducers of pro-inflammatory and pro-regenerative phenotypes, respectively, for 3 hours and assessed for the expression of pro-inflammatory- or pro-regenerative genes. Interestingly, the mRNA levels of pro-inflammatory genes, IL-1β and IL-6, which were similar at basal condition, were significantly increased in macrophages isolated from LysM-Cre:$MCT^{f/f}$ compared to $MCT^{f/f}$ mice after stimulation with LPS plus IFN-γ (Figure 5, G and H). In contrast, the expression of pro-regenerative gene Arg-1, which was also similar at basal condition, was lower in macrophages isolated from LysM-Cre:$MCT^{f/f}$ compared to $MCT^{f/f}$ mice after stimulation with IL-4 (Figure 5I). Other genes that have been associated with specific macrophage phenotypes (i.e., pro-inflammatory gene TNF-α and pro-regenerative gene Ym-1) were independent of MCT1 expression after this acute stimulation with pro-inflammatory and pro-regenerative phenotype inducers (Supplemental Figure 9, A and B). A critical function of macrophages in nerve regeneration is to phagocytose axonal and myelin debris (19). Thus, we also examined the impact of MCT1 deficiency on the phagocytic activity of macrophages at basal condition. We found that the MCT1-deficient macrophages have significantly lower phagocytic capacity than the macrophages isolated from littermate control mice (Figure 5, J and K). To investigate the

mechanism, we evaluated the expression of phagocytosis-associated genes in macrophages isolated from wild-type and LysM-Cre:MCT1$^{f/f}$ mice. Although the expression of phagocytosis-associated surface receptors, namely mannose receptor (CD206), complement receptor 3 (CR3), scavenger receptor macrophage receptor with collagenous structure (MARCO), and macrophage scavenger receptor 1 (MSR-1), were unchanged (Supplemental Figure 10, A to D), macrophages isolated from LysM-Cre:MCT1$^{f/f}$ mice revealed significant reduction in expression of milk fat globule factor-E8 (MFG-E8) compared with macrophages isolated from littermate control mice (Figure 5L). MFG-E8 is expressed and secreted by phagocytes, including macrophages, and it promotes phagocytosis by specifically binding to apoptotic cells through recognition of aminophospholipids such as phosphatidylserine, which is the key "eat-me" signal exposed on the surface of apoptotic cells (60). In addition, MFG-E8 favors wound healing by reprograming macrophages from pro-inflammatory to pro-regenerative phenotype and enhancing the production of basic fibroblast growth factor (61). In support of these *in vitro* results, we found that MCT1 deficiency significantly reduced the engulfment of myelin debris by macrophages in sciatic nerves from injured mice (Supplemental Figure 11, A and B). Our results suggest that MCT1 deficiency in macrophages impairs the signaling cascade responsible for specific recognition of apoptotic cells by phagocyte receptors, providing a novel insight into the MCT1-mediated mechanism of phagocytosis. Taken together, these findings indicate that MCT1 is an important determinant of macrophage phenotype during inflammation, both for shaping the cytokine microenvironment and contributing to the critical function of macrophage phagocytosis.

MCT1-regulated macrophage phenotypes and functions in injured nerves are potentially determined through ATF3

Given the remarkable impact of MCT1 deficiency on inflammatory cytokine expression *in vivo* (injured sciatic nerve) and *in vitro* (cultured macrophages), we analyzed the effect of macrophage-specific MCT1 deficiency on the expression of ATF3, a general injury-inducible transcription factor and a repressor for sustained expression of several inflammatory genes in macrophages (62-64). We found that stimulation of macrophages with the M1-inducer, LPS+IFN-γ, for 6 hours reduced the expression of ATF3, which subsequently resolved following 24 hours in control macrophage cultures. In contrast to wild-type $MCT1^{f/f}$ mice, ATF3 expression did not return to normal in peritoneal exudative macrophages isolated from LysM Cre:$MCT1^{f/f}$ mice (Figure 6, A and B). Consistent with these *in vitro* findings, ATF3 expression was also significantly decreased in injured sciatic nerves from mice with macrophage-specific MCT1 deletion (Figure 6, C and D). These findings suggest that MCT1 deletion in macrophages decreases the expression of ATF3, leading to an increase in expression of proinflammatory cytokines and impaired nerve regeneration (Figure 6E).

Adoptive cell transfer of macrophages with intact MCT1 completely repairs impaired nerve regeneration in macrophage-specific MCT1 knockout mice

Adoptive cell transfer of chimeric antigen receptor-modified T cells (i.e., CAR-T cells) is now well established for treatment of hematologic malignancies (65) and is being considered for solid tumors, infections, and autoimmune conditions (66, 67). To date, adoptive cell transfer of macrophages has proven safe, but not yet effective, in treating cancer patients (68). Understanding of nerve degeneration and regeneration has been broadened by studies performing bone marrow transplants (69) and parabiosis (70) in mouse models. Though adoptive cell transfer of macrophages has previously been published in rat model of neuropathic pain (71) and

other non-neurologic mouse models (72, 73), evaluating the impact of adoptive cell transfer of macrophages on regeneration from peripheral nerve injury has never previously been reported. First, we confirmed that macrophages injected intravenously would target crushed sciatic nerve. Bone marrow-derived macrophages (BMDMs) obtained from Bl6:LysM-Cre:RosaYFP mice were injected into the tail-vein of control Bl6 mice 3 days following unilateral sciatic nerve crush. BMDMs, which express macrophage marker F4/80, targeted and survived in injured, but not uninjured, sciatic nerves (Figure 7, A to C). We chose to inject BMDMs 3 days following sciatic nerve crush because this is the timepoint when circulating macrophages infiltrate the injured nerve (7). To measure the impact of adoptive cell transfer of macrophages on nerve regeneration, we backcrossed MCT1$^{f/f}$ mice for 8 generations to C57Bl/6J mice and mated them with B6:LysM-Cre mice to produce macrophage-specific MCT1 knockout mice on C57BL/6J background (B6: LysM-Cre: MCT1$^{f/f}$). Following sciatic nerve crush, Bl6: LysM-Cre: MCT1$^{f/f}$ and wild-type mice showed similar impairment in nerve regeneration, as measured by electrophysiology (Figure 7, D to F), as the mixed background LysM-Cre: MCT1$^{f/f}$ and MCT1$^{f/f}$ mice investigated previously (Figure 1). Lack of exact overlap between data sets (wild-type/floxed littermate control versus macrophage-specific MCT1 knockout mice in Figure 1, C and D and Figure 7, E and F) may be due to differences in sample size and strain backgrounds. Additionally, and more importantly, tail-vein injection of BMDMs derived from C57BL/6J wild-type mice led to complete recovery of the impaired regeneration in B6: LysM-Cre: MCT1$^{f/f}$ mice, while having no impact on C57Bl6 wild-type mice. These results confirm that the ablation of MCT1 within macrophages was responsible for the impaired regeneration in B6: LysM-Cre: MCT1$^{f/f}$ mice. They also suggest that adoptive cell transfer of macrophages may be a useful strategy for treating nerve injuries in patients.

MCT1 overexpression in macrophages accelerates peripheral nerve regeneration

The experiments in transgenic mice and macrophage cultures with ablation of macrophage MCT1 are critical for advancing our knowledge of the specific role this transporter plays in macrophage cell biology and nerve regeneration. To explore the translational significance of these findings, we tested peripheral nerve regeneration in transgenic mice with upregulated expression of MCT1 only in macrophages. Tet-inducible MCT1 overexpressor mice ($MCT1^{Over/WT}$), which were previously published (74), were mated with ROSA:LNL:tTA (tTA; from Jackson Laboratories) and LysM-Cre mice to produce LysM-Cre:$tTA^{+/-}$:$MCT1^{Over/+}$ and littermate control ($MCT1^{Over/WT}$) mice (Figure 8A). Macrophages isolated from these mice had increased MCT1 expression (Figure 8B) and lactate transport (Figure 8C) compared to littermate controls. We confirmed that MCT1 mRNA expression in control mice macrophages isolated from the overexpressor mice ($MCT1^{Over/WT}$) were not significantly different from that of the knockout mice ($MCT1^{f/f}$) (data not shown). LysM-Cre:$tTA^{+/-}$:$MCT1^{Over/+}$ mice have improved nerve regeneration following crush compared to $MCT1^{Over/+}$ mice, as measured by electrophysiology (Figure 8, D and E), neuromuscular junction (NMJ) reinnervation (Figure 8, F and G), and myelinated axon counts (Figure 8, H and I and Supplemental Figure 12). Like macrophage-specific MCT1 deficient mice (Supplemental Figure 5), transgenic mice having macrophage selective MCT1 overexpression had unchanged motor (Supplemental Figure 13, A and B) or sensory (Supplemental Figure 13, C and D) behavioral recovery following sciatic nerve injury, as compared with their littermate controls. These experiments make it clear that macrophage MCT1 is not only necessary for nerve regeneration, but upregulation of this transporter can accelerate nerve regeneration and may potentially be a target for treatment of nerve injuries in patients.

Discussion

Despite having the capacity to regenerate, the functional recovery following peripheral nerve injury is slow and often incomplete (6). Though macrophages have been known to participate in peripheral nerve regeneration and repair for decades (12, 22, 75, 76), almost nothing is known about the role that intracellular metabolism plays in this function. Several seminal studies published recently indicate that macrophage function, at least *in vitro*, is dependent on specific alteration of macrophage intracellular metabolism (25, 28, 77-83). Combining an analysis of macrophage intracellular metabolism and immune responses, along with its impact on an experimental model of peripheral nerve regeneration, we find that MCT1 is an important contributor to macrophage cellular function and their biologic role in recovery from nerve injury. Our results also suggest that MCT1 in DRG neurons, Schwann cells, and perineurial cells is not involved in peripheral nerve regeneration. It should be noted that all of these cell types express more than one MCT, and thus, the lack of impact from eliminating just MCT1 does not preclude an effect from other MCTs, either as the primary transporter involved in nerve regeneration or in compensation for the lack of MCT1. Thus, a recent study demonstrating the importance of Schwann cell glycolysis and release of lactate to the support of regenerating axons is likely due to MCT4, either alone or combined with MCT1, rather than MCT1 alone (84, 85).

The distinct functional states of macrophages depend on their intracellular metabolic program, which is governed by the cross-talk between intracellular signaling cascades, metabolic mediators, and their metabolites (24-27, 77-83, 86). Emerging evidence suggests that immune effector functions, particularly cytokine production, are directly coupled to specific changes in

cellular metabolism (29). Macrophages stimulated *in vitro* to a pro-inflammatory state have blockade of the TCA cycle at two sites, causing a reduction of oxidative metabolism and simultaneous upregulation of genes that mediate the pentose phosphate pathway, glycolysis, and lactate production in order to produce sufficient ATP for cell survival (25). In contrast, macrophages stimulated *in vitro* to a pro-regenerative state upregulate glycolysis and fatty acid oxidation to support an activated TCA cycle (25). Our findings suggest that MCT1 is an important mediator of macrophage intracellular metabolism and function. Both glycolysis and mitochondrial metabolism are impaired in macrophages with conditionally-ablated MCT1. Additionally, macrophages without MCT1 have increased expression of pro-inflammatory and decreased expression of pro-regenerative cytokines. This was observed both in macrophages isolated *in vitro* and in peripheral nerve following nerve injury. Finally, ablation of MCT1 from macrophages reduces their phagocytic capacity, both in culture and in injured nerves, by impairing the specific recognition of apoptotic cells by phagocyte receptors. Given the recently identified role of MCT1 and lactate in macrophage efferocytosis (83), which is the engulfment of dead or injured cells, the phagocytosis of axons and myelin may also similarly be dependent on this transporter. Interestingly, not all functions of macrophages are impacted by loss of MCT1, as macrophage survival, migration, and infiltration of the injured nerve is not altered in LysM-Cre: $MCT1^{f/f}$ mice. The disruption of these critical functions of macrophages, particularly cytokine production and phagocytosis, likely contribute to the disruption of peripheral nerve regeneration observed in LysM-Cre:$MCT1^{f/f}$ mice.

ATF3 is well known for its function as the inducible repressor for sustained expression of several inflammatory genes in macrophages (62, 63). Furthermore, ATF3, a general injury-inducible factor, plays a pro-regenerative role during peripheral nerve regeneration (64). In this

study, cultured macrophages having ablated MCT1 show decreased expression of ATF3 after chronic exposure with M1 phenotype inducers. Consistent with these *in vitro* observations, injured sciatic nerves from macrophage-specific MCT1 deficient mice shows decreased expression of ATF3. These findings suggest that ATF3 plays an important role in MCT1-mediated cellular and biologic functions of macrophages. Deficiency of MCT1 represses ATF3 expression, promotes the proinflammatory state of macrophages, and adversely affects the recovery from nerve injury.

To date, there are no approved therapies for accelerating nerve regeneration (22) and patients with proximal nerve injuries, from either trauma or other conditions, have little hope of functional improvement since unaided peripheral nerve regeneration is slow and incomplete. Besides evaluating the impact of ablating MCT1 from macrophages *in vitro* and *in vivo*, we, for the first time, demonstrate that manipulating macrophage metabolism can actually accelerate peripheral nerve regeneration. Using conditional transgenic mice that upregulate MCT1 only in macrophages, we show acceleration of nerve regeneration with clear improvements in both CMAP amplitude and NMJ reinnervation, which are electrophysiologic and histologic markers for successful axon regeneration, respectively. These studies suggest that upregulation of macrophage MCT1, or perhaps other metabolic targets, is an exciting pathway that could potentially be manipulated in patients to treat peripheral nerve injuries.

Interestingly, but perhaps not surprisingly, we did not see the expected impact of macrophage-specific MCT1 down/up-regulation on behavioral measures of recovery following sciatic nerve injury. For some measures, in fact, we saw the opposite impact than we expected. We have identified the following three possible reasons for this discrepancy: First, axonal

regeneration, remyelination, nerve conduction, and behavioral recoveries are controlled by different and mostly independent mechanisms. The behavioral recovery happens very quickly, which make it difficult to identify any improvements in the macrophage-specific MCT1 overexpressing mice. Second, sensitivity to mechanical and thermal stimuli is not only mediated by peripheral axons. The microenvironment of the DRG also plays an important role in this behavior. DRGs are reported to contain populations of self-renewing cells, collectively referred to as DRG resident cycling cells, that are active not only in "quiescent" ganglia but also accelerate their turnover in response to distal axotomy (87). A recent study employing spared nerve injury model of neuropathic pain in mice reports that macrophages in the DRG, but not at the peripheral nerve injury site, are critical contributors to maintenance of the peripheral nerve injury-induced hypersensitivity (88). Third, the impact of macrophages on muscle atrophy and regeneration, which will impact motor behavior recovery, may not be the same as the impact on peripheral nerves. A recent publication showed that lactate and macrophage MCT1 plays a direct role in muscle revascularization and regeneration following ischemia (83). This independent impact of macrophage MCT1 on muscle, as opposed to the changes seen in nerve regeneration, may drive the motor behavioral measures evaluated in this study.

Thus far, virtually all of the efforts to improve nerve regeneration have focused on neurons and Schwann cells. Though some genes have been found to accelerate nerve regeneration, described as regeneration-associated genes or RAGs (89, 90), these genes have not been clinically useful targets due to being known oncogenes. In contrast to these studies, MCT1 is not an oncogene, and the focus on macrophages is novel. Unlike neurons and Schwann cell, for which there are no easy techniques for effective transplantation, macrophages are a cell type that can be safely transfused into patients. In fact, we demonstrate for the first time the feasibility

of macrophage adoptive cell transfer for the treatment of peripheral nerve injuries. Given this, it is not far-fetched to imagine treating acute peripheral nerve injuries in patients with infusion of macrophages that have been isolated from patients and modified to upregulate MCT1 or other targets to alter their cellular metabolism and function. The field of immunometabolism is very exciting and has thus far primarily been focused on cancer therapeutics. The experiments detailed here should open up the field to other disciplines and may represent the first of many medical conditions being amenable to treatment with metabolically altered macrophages.

Methods

Experimental design. All experiments were performed using male or female littermate mice (~100 days old, n = 3 to 13 per group as indicated in figure legends). Samples sizes were chosen based on previous expertise, knowledge from past experiments and statistical considerations using similar model systems (cell culture and mouse studies), and current accepted standards based on literature review. Investigators performing the surgeries, electrophysiologic recordings, quantitative histological staining, behavioral assessments, and morphometric analyses were blinded to mice genotype or treatment. The findings in this study were collected from multiple independent experiments and were reliably reproduced. Analysis was performed without knowledge of experimental group assignment, and we did not exclude any data from the study.

Animals. Our lab-developed MCT1$^{f/f}$ mice (40) were bred with transgenic mice with Cre recombinase driven by LysM-Cre (Jackson Laboratory; stock no: 004781), P0-Cre (Jackson Laboratory; stock no. 017927), Adv-Cre (91), and Gli1-CreER^{T2} (Jackson Laboratory; stock no. 007913) to generate cell-specific ablation of MCT1 from macrophages (LysM-Cre:MCT1$^{f/f}$), Schwann cells (P0-Cre:MCT1$^{f/f}$), DRG neurons (Adv-Cre:MCT1$^{f/f}$), or perineurial cells (Gli1-

Cre^{ERT2}:$MCT1^{f/f}$) and littermate controls. With the exception of the adoptive cell transfer experiments, the mice in all experiments were of mixed background composed of C57Bl6 and SJL mice. For the experiments using mice of mixed background, only littermates were used to minimize variability in the results of those experiments. As stated in the results, both mixed and C57Bl6 congenic background mice had similarly delayed nerve regeneration following ablation of macrophage MCT1. Gli1- Cre^{ERT2}:$MCT1^{f/f}$ mice were treated with tamoxifen (125 mg/kg/body weight, i.p.) every alternate day over 7 days at approximately 2 months of age, as described previously (92), to induce recombination of MCT1 gene. Gli1- Cre^{ERT2}:$MCT1^{f/f}$ mice were used for studies at least two weeks after tamoxifen treatment. Animals were monitored for adverse effects of treatment, but none were noted during or after the course of treatment that required euthanasia. Transgenic mice with upregulation of MCT1 selectively in macrophages (LysM-Cre:$tTA^{+/-}$:$MCT1^{Over/+}$) were produced by crossing LysM-Cre mice with ROSA LNL tTA (tet-off) mice (Jackson Laboratory; stock no: 011008) and a tet-responsive MCT1 overexpressor mouse ($MCT1^{Over/+}$ (74)). Genotypes for knockout or overexpressor mice and littermate control mice were performed as described previously (40, 93) and/or by using the protocols obtained from the providers. At baseline, none of these knockout, overexpressor, or littermate control mice showed any signs of peripheral neuropathy.

Sciatic nerve crush. All surgical experiments were performed under 2% isoflurane on adult male or female littermate mice (~100 days old). As published previously (38, 94), sciatic nerve crush injury was performed by exposing right sciatic nerve at mid-thigh level, crushing sciatic nerve with smooth forceps for 20 seconds, closing the skin incision with surgical staples, and allowing the animals to recover on a warming blanket.

Nerve conduction studies. Electrophysiologic recordings were performed to measure CMAPs by using a Neurosoft-Evidence 3102evo electromyograph system (Schreiber & Tholen Medizintechnik, Stade, Germany). During all recording sessions, mice were anesthetized with 2% isoflurane and positioned face down. CMAPs were determined by placing stimulating electrodes (27G stainless steel needle electrodes, Natus Medical, Inc., San Carlos, CA) at the sciatic notch and Achilles tendon, and recording electrodes in the lateral plantar muscles of the foot. Stimulation of each nerve segment was performed, with increasing voltage, until the maximal response was achieved, as evidenced by no further increase or decrease in CMAP amplitude, despite an increase in stimulation voltage. Nerves were stimulated by very short (<0.2 ms) electrical impulses. Response latency for each proximal or distal stimulation was measured from stimulus onset, and peak-to-peak amplitudes were calculated. Motor NCV was calculated by dividing the distance between sciatic notch and Achilles tendon by the difference between the response latencies. The distance between sciatic notch and Achilles tendon, which was mostly in the range of 24–26 mm, was measured for each mouse at each electrophysiological recording session using geometrical divider and scale. Unless otherwise stated, all nerve conduction studies were conducted at room temperature.

Mouse behavioral assessments. Motor behaviors were assessed by measuring toe spread index (TSI) (94) and hindlimb grip strength (95) as described previously. For TSI, mice were gently covered with a piece of cloth and lifted by the tail, uncovering the hind paws for clear observation, and rapidly turned over to expose their ventral side. These conditions caused the toe spreading reflex and the amount of digit spread was observed. This parameter was graded from 0 (no active spreading of any toes) to 2 (active spreading of all toes), with 1 being assigned to intermediate spreading of toes. The toe spreading reflex is dependent on innervation of the small

muscles of the foot and thus correlates with reinnervation and muscle regrowth following nerve injury. Hindlimb grip strength was measured on a Chatillon force gauge meter (Ametek, Largo) and recorded as the best of three values within 2 minutes. Sensory behaviors were assessed using pinprick and brush tests as described previously (94, 96). Briefly, for pinprick test, mice were habituated for at least 20 minutes on wire mesh cages. After the habituation, an Austerlitz insect pin (size, 000; Fine Scientific Tools) was gently applied to the plantar surface of the paw without skin penetration. The most lateral part of the plantar surface of the hind paw (sensory field of the sciatic nerve) was divided into 5 areas. The pinprick was applied from the most lateral toe to the heel. A response was considered positive when the animal briskly removed its paw, and the animal was graded 1 for this area, and then tested for the next one. If none of the applications elicited a positive response, the overall grade was 0. In that case, the saphenous territory of the same paw was tested as a positive control, which always elicited a positive response. For brush test, the plantar hindpaw of mice habituated on wire mesh cages for 30 min was stimulated by light stroking from heel to toe with a round-head paintbrush with a diameter of 2mm (Princeton Brush Co.) onto the sural territory of the paw separated into two halves. Each series of stimulations started at the distal part of the paw to its middle and lasted less than 1 s. The brush was applied twice in each territory and the mouse was scored 1 per territory if it withdrew its paw upon stimulation.

Seahorse bioenergetic analysis. Peritoneal exudate macrophages were used for measurements of oxygen consumption and extracellular acidification using XF96 extracellular flux analyzer (Seahorse Bioscience, North Billerica, MA) following the manufacturer's instructions (97). Macrophages were plated at 10,000 cells/well on Seahorse XF96 cell culture microplates in DMEM/F12 media with 5.5 mM D-glucose for 24 hours. Bioenergetic analysis was performed

by sequentially injecting 2 μM oligomycin, 4 μM carbonyl cyanide *p*-(trifluoromethoxy) phenylhydrazone (FCCP), 0.5 μM rotenone and 4 μM antimycin. Data are expressed as oxygen consumption rate (OCR) in picomole per minute and extracellular acidification rate (ECAR) in milli pH per minute for 10,000 cells. Total ATP generated from oxidative metabolism was estimated by the following formula: $ATP_{oxid} = (OCR_{mito} \times P/O_{TCA} + OCR_{coupled} \times P/O_{oxid}) \times 2$. $OCR_{mito} = OCR_{total} - OCR_{rot}$. P/O_{TCA} *ratio is 0.121.* $OCR_{coupled} = (OCR_{total} - OCR_{oligo}) \times 0.908$. P/O_{oxid} *ratio is 2.486.* Total ATP generated from glycolysis was estimated by the following formula: $ATP_{glyc} = PPR_{glyc} + OCR_{mito} \times 2ATP/lactate \times P/O_{glyc}$. $PPR_{glyc} = PPR_{tot} - PPR_{resp}$. $PPR_{tot} = ECAR \times 0.1$ *(buffering power for DMEM).* $PPR_{resp} = (10^{(pH-pK)}/1+10^{(pH-pK)}) \times OCR_{mito}$. *ATP/lactate = 1.* P/O_{glyc} *ratio is 0.242. oxid*; oxidative phosphorylation; *mito*: mitochondrial; *P/O ratio*: yield of ATP per Oxygen atom consumed; *rot*: rotenone; *TCA*: tricarboxylic acid cycle; *oligo*: oligomycin; *PPR*: proton production rate. The rationale and explanation for these formulas has been published previously (98-100).

Adoptive cell transfer of bone marrow-derived macrophages (BMDMs). BMDMs were generated as described previously (101). Briefly, bone marrow cell suspension was prepared by flushing bone marrow with DMEM supplemented with 10% fetal bovine serum (FBS), 1% penicillin/streptomycin and 2 mM L-glutamine plus 20% L929-conditioned medium. The cells were incubated at 37°C and 5% CO_2 atmosphere, and on day 4, non-adherent cells were removed and the medium was replenished. On day 7, BMDMs were lifted using Cellstripper (Mediatech, Manassas, VA) and dispersed in PBS. BMDMs (5×10^6 cells/100 μL/mouse) were injected via tail vein 3 days after sciatic nerve crush.

Statistics. Analyses were performed blinded to animal genotype and treatment. Although we did not perform statistical tests to predetermine sample size, our samples sizes are similar to previously published studies in the field. Statistical analyses were performed with GraphPad Prism 8 (GraphPad Software) by using unpaired *t* test with two tails with unequal variance or two-way ANOVA with post hoc test when required conditions were met. The number of animals per group or independent repeats (*n*), the statistical test used for comparison, and the statistical significance (*p* value) was stated for each figure panel in the respective legend. All data were presented as the mean ± *SEM* unless otherwise noted. Differences in the *P* values of <0.05 were considered statistically significant.

Study approval. All animal experiments were carried out in compliance with the protocols approved by the Johns Hopkins University Institutional Animal Care and Use Committee (IACUC).

Additional methods are available as *Supplemental Material*

Author contributions

M.K.J. designed and performed experiments, analyzed data, and wrote the manuscript. J.V.P., A.R., X.H.A., F.Y., S.V., and A.L. performed some of the experiments. S.L.C., M.R.H., A.H., G.A.R., and J.D.R. assisted with resources and/or provided expertise and feedback. B.M.M. secured funding, designed and supervised the study, analyzed data, and wrote the manuscript. B.M.M. is the guarantor of this work and, as such, has full access to all the data in the study and takes responsibility for the integrity of the data and the accuracy of the data analysis. All authors approved the final manuscript.

Acknowledgements

The authors would like to thank Dr. Mohamed Farah, Ms. Kimberly Brown, Carol Cooke, and the Johns Hopkins Neurology Electron Microscopy Core for their assistance in processing embedded nerve tissue for toluidine blue staining, photographing electron microscopy images, and assisting with interpretation. We would also like to thank Drs. Weiran Chen, Research Associate Johns Hopkins School of Medicine, and Yagendra Nadava, Visiting Assistant Professor at University of Maryland School of Medicine, for their assistance in generating and interpreting SeaHorse Bioanalyzer data. Financial support was provided by NIH-NS086818-01 (B.M.M.) and R01NS112266 (A.L). G.A.R. was supported by a Wellcome Trust Investigator Award (WT212625/Z/18/Z) and MRC Programme grant (MR/R022259/1).

References

1. Conforti L, Gilley J, and Coleman MP. Wallerian degeneration: an emerging axon death pathway linking injury and disease. *Nat Rev Neurosci*. 2014;15(6):394-409.
2. Cattin AL, and Lloyd AC. The multicellular complexity of peripheral nerve regeneration. *Curr Opin Neurobiol*. 2016;39:38-46.
3. Stierli S, Imperatore V, and Lloyd AC. Schwann cell plasticity-roles in tissue homeostasis, regeneration, and disease. *Glia*. 2019.
4. Godzik K, and Coleman MP. The axon-protective WLD(S) protein partially rescues mitochondrial respiration and glycolysis after axonal injury. *J Mol Neurosci*. 2015;55(4):865-71.
5. Geisler S, Huang SX, Strickland A, Doan RA, Summers DW, Mao X, et al. Gene therapy targeting SARM1 blocks pathological axon degeneration in mice. *J Exp Med*. 2019;216(2):294-303.
6. Scheib J, and Hoke A. Advances in peripheral nerve regeneration. *Nat Rev Neurol*. 2013;9(12):668-76.
7. Gaudet AD, Popovich PG, and Ramer MS. Wallerian degeneration: gaining perspective on inflammatory events after peripheral nerve injury. *J Neuroinflammation*. 2011;8:110.
8. Wujek JR, and Lasek RJ. Correlation of axonal regeneration and slow component B in two branches of a single axon. *J Neurosci*. 1983;3(2):243-51.
9. Brushart TM, Hoffman PN, Royall RM, Murinson BB, Witzel C, and Gordon T. Electrical stimulation promotes motoneuron regeneration without increasing its speed or conditioning the neuron. *J Neurosci*. 2002;22(15):6631-8.
10. Redett R, Jari R, Crawford T, Chen YG, Rohde C, and Brushart TM. Peripheral pathways regulate motoneuron collateral dynamics. *J Neurosci*. 2005;25(41):9406-12.
11. Jonsson S, Wiberg R, McGrath AM, Novikov LN, Wiberg M, Novikova LN, et al. Effect of delayed peripheral nerve repair on nerve regeneration, Schwann cell function and target muscle recovery. *PLoS One*. 2013;8(2):e56484.
12. Chen P, Piao X, and Bonaldo P. Role of macrophages in Wallerian degeneration and axonal regeneration after peripheral nerve injury. *Acta Neuropathol*. 2015;130(5):605-18.
13. Bruck W. The role of macrophages in Wallerian degeneration. *Brain Pathol*. 1997;7(2):741-52.
14. Stratton JA, Holmes A, Rosin NL, Sinha S, Vohra M, Burma NE, et al. Macrophages Regulate Schwann Cell Maturation after Nerve Injury. *Cell Rep*. 2018;24(10):2561-72 e6.
15. DeFrancesco-Lisowitz A, Lindborg JA, Niemi JP, and Zigmond RE. The neuroimmunology of degeneration and regeneration in the peripheral nervous system. *Neuroscience*. 2015;302:174-203.
16. Mokarram N, and Bellamkonda RV. A perspective on immunomodulation and tissue repair. *Ann Biomed Eng*. 2014;42(2):338-51.
17. Kolter J, Feuerstein R, Zeis P, Hagemeyer N, Paterson N, d'Errico P, et al. A Subset of Skin Macrophages Contributes to the Surveillance and Regeneration of Local Nerves. *Immunity*. 2019;50(6):1482-97 e7.
18. La Fleur M, Underwood JL, Rappolee DA, and Werb Z. Basement membrane and repair of injury to peripheral nerve: defining a potential role for macrophages, matrix

metalloproteinases, and tissue inhibitor of metalloproteinases-1. *J Exp Med*. 1996;184(6):2311-26.
19. Liu P, Peng J, Han GH, Ding X, Wei S, Gao G, et al. Role of macrophages in peripheral nerve injury and repair. *Neural Regen Res*. 2019;14(8):1335-42.
20. Tomlinson JE, Zygelyte E, Grenier JK, Edwards MG, and Cheetham J. Temporal changes in macrophage phenotype after peripheral nerve injury. *J Neuroinflammation*. 2018;15(1):185.
21. Siqueira Mietto B, Kroner A, Girolami EI, Santos-Nogueira E, Zhang J, and David S. Role of IL-10 in Resolution of Inflammation and Functional Recovery after Peripheral Nerve Injury. *J Neurosci*. 2015;35(50):16431-42.
22. Zigmond RE, and Echevarria FD. Macrophage biology in the peripheral nervous system after injury. *Prog Neurobiol*. 2019;173:102-21.
23. Nadeau S, Filali M, Zhang J, Kerr BJ, Rivest S, Soulet D, et al. Functional recovery after peripheral nerve injury is dependent on the pro-inflammatory cytokines IL-1beta and TNF: implications for neuropathic pain. *J Neurosci*. 2011;31(35):12533-42.
24. O'Neill LA, Kishton RJ, and Rathmell J. A guide to immunometabolism for immunologists. *Nat Rev Immunol*. 2016;16(9):553-65.
25. Jha AK, Huang SC, Sergushichev A, Lampropoulou V, Ivanova Y, Loginicheva E, et al. Network integration of parallel metabolic and transcriptional data reveals metabolic modules that regulate macrophage polarization. *Immunity*. 2015;42(3):419-30.
26. Ouimet M, Ediriweera HN, Gundra UM, Sheedy FJ, Ramkhelawon B, Hutchison SB, et al. MicroRNA-33-dependent regulation of macrophage metabolism directs immune cell polarization in atherosclerosis. *J Clin Invest*. 2015;125(12):4334-48.
27. Netea MG, Joosten LA, van der Meer JW, Kullberg BJ, and van de Veerdonk FL. Immune defence against Candida fungal infections. *Nat Rev Immunol*. 2015;15(10):630-42.
28. Langston PK, Shibata M, and Horng T. Metabolism Supports Macrophage Activation. *Front Immunol*. 2017;8:61.
29. Diskin C, and Palsson-McDermott EM. Metabolic Modulation in Macrophage Effector Function. *Front Immunol*. 2018;9:270.
30. Byles V, Covarrubias AJ, Ben-Sahra I, Lamming DW, Sabatini DM, Manning BD, et al. The TSC-mTOR pathway regulates macrophage polarization. *Nat Commun*. 2013;4:2834.
31. Covarrubias AJ, Aksoylar HI, Yu J, Snyder NW, Worth AJ, Iyer SS, et al. Akt-mTORC1 signaling regulates Acly to integrate metabolic input to control of macrophage activation. *Elife*. 2016;5.
32. Biswas SK, and Mantovani A. Orchestration of metabolism by macrophages. *Cell Metab*. 2012;15(4):432-7.
33. Murray CM, Hutchinson R, Bantick JR, Belfield GP, Benjamin AD, Brazma D, et al. Monocarboxylate transporter MCT1 is a target for immunosuppression. *Nat Chem Biol*. 2005;1(7):371-6.
34. Ekberg H, Qi Z, Pahlman C, Veress B, Bundick RV, Craggs RI, et al. The specific monocarboxylate transporter-1 (MCT-1) inhibitor, AR-C117977, induces donor-specific suppression, reducing acute and chronic allograft rejection in the rat. *Transplantation*. 2007;84(9):1191-9.

35. Haas R, Smith J, Rocher-Ros V, Nadkarni S, Montero-Melendez T, D'Acquisto F, et al. Lactate Regulates Metabolic and Pro-inflammatory Circuits in Control of T Cell Migration and Effector Functions. *PLoS Biol*. 2015;13(7):e1002202.
36. Zhang J, Muri J, Fitzgerald G, Gorski T, Gianni-Barrera R, Masschelein E, et al. Endothelial Lactate Controls Muscle Regeneration from Ischemia by Inducing M2-like Macrophage Polarization. *Cell Metab*. 2020;31(6):1136-53 e7.
37. Watson MJ, Vignali PDA, Mullett SJ, Overacre-Delgoffe AE, Peralta RM, Grebinoski S, et al. Metabolic support of tumour-infiltrating regulatory T cells by lactic acid. *Nature*. 2021.
38. Morrison BM, Tsingalia A, Vidensky S, Lee Y, Jin L, Farah MH, et al. Deficiency in monocarboxylate transporter 1 (MCT1) in mice delays regeneration of peripheral nerves following sciatic nerve crush. *Exp Neurol*. 2015;263:325-38.
39. Halestrap AP. The SLC16 gene family - structure, role and regulation in health and disease. *Mol Aspects Med*. 2013;34(2-3):337-49.
40. Jha MK, Lee Y, Russell KA, Yang F, Dastgheyb RM, Deme P, et al. Monocarboxylate transporter 1 in Schwann cells contributes to maintenance of sensory nerve myelination during aging. *Glia*. 2020;68(1):161-77.
41. Tofaris GK, Patterson PH, Jessen KR, and Mirsky R. Denervated Schwann cells attract macrophages by secretion of leukemia inhibitory factor (LIF) and monocyte chemoattractant protein-1 in a process regulated by interleukin-6 and LIF. *J Neurosci*. 2002;22(15):6696-703.
42. Namikawa K, Okamoto T, Suzuki A, Konishi H, and Kiyama H. Pancreatitis-associated protein-III is a novel macrophage chemoattractant implicated in nerve regeneration. *J Neurosci*. 2006;26(28):7460-7.
43. Napoli I, Noon LA, Ribeiro S, Kerai AP, Parrinello S, Rosenberg LH, et al. A central role for the ERK-signaling pathway in controlling Schwann cell plasticity and peripheral nerve regeneration in vivo. *Neuron*. 2012;73(4):729-42.
44. Abram CL, Roberge GL, Hu Y, and Lowell CA. Comparative analysis of the efficiency and specificity of myeloid-Cre deleting strains using ROSA-EYFP reporter mice. *J Immunol Methods*. 2014;408:89-100.
45. Shi J, Hua L, Harmer D, Li P, and Ren G. Cre Driver Mice Targeting Macrophages. *Methods Mol Biol*. 2018;1784:263-75.
46. Clausen BE, Burkhardt C, Reith W, Renkawitz R, and Forster I. Conditional gene targeting in macrophages and granulocytes using LysMcre mice. *Transgenic Res*. 1999;8(4):265-77.
47. Hume DA. Applications of myeloid-specific promoters in transgenic mice support in vivo imaging and functional genomics but do not support the concept of distinct macrophage and dendritic cell lineages or roles in immunity. *J Leukoc Biol*. 2011;89(4):525-38.
48. Merezhinskaya N, Ogunwuyi SA, Mullick FG, and Fishbein WN. Presence and localization of three lactic acid transporters (MCT1, -2, and -4) in separated human granulocytes, lymphocytes, and monocytes. *J Histochem Cytochem*. 2004;52(11):1483-93.
49. Lindborg JA, Mack M, and Zigmond RE. Neutrophils Are Critical for Myelin Removal in a Peripheral Nerve Injury Model of Wallerian Degeneration. *J Neurosci*. 2017;37(43):10258-77.

50. Perkins NM, and Tracey DJ. Hyperalgesia due to nerve injury: role of neutrophils. *Neuroscience*. 2000;101(3):745-57.
51. Lindborg JA, Niemi JP, Howarth MA, Liu KW, Moore CZ, Mahajan D, et al. Molecular and cellular identification of the immune response in peripheral ganglia following nerve injury. *J Neuroinflammation*. 2018;15(1):192.
52. Sykes DB, Scheele J, Pasillas M, and Kamps MP. Transcriptional profiling during the early differentiation of granulocyte and monocyte progenitors controlled by conditional versions of the E2a-Pbx1 oncoprotein. *Leuk Lymphoma*. 2003;44(7):1187-99.
53. Raes G, Van den Bergh R, De Baetselier P, Ghassabeh GH, Scotton C, Locati M, et al. Arginase-1 and Ym1 are markers for murine, but not human, alternatively activated myeloid cells. *J Immunol*. 2005;174(11):6561; author reply -2.
54. Monaco S, Gehrmann J, Raivich G, and Kreutzberg GW. MHC-positive, ramified macrophages in the normal and injured rat peripheral nervous system. *J Neurocytol*. 1992;21(9):623-34.
55. Wang PL, Yim AKY, Kim KW, Avey D, Czepielewski RS, Colonna M, et al. Peripheral nerve resident macrophages share tissue-specific programming and features of activated microglia. *Nat Commun*. 2020;11(1):2552.
56. Chavan SS, Pavlov VA, and Tracey KJ. Mechanisms and Therapeutic Relevance of Neuro-immune Communication. *Immunity*. 2017;46(6):927-42.
57. Carr MJ, Toma JS, Johnston APW, Steadman PE, Yuzwa SA, Mahmud N, et al. Mesenchymal Precursor Cells in Adult Nerves Contribute to Mammalian Tissue Repair and Regeneration. *Cell Stem Cell*. 2019;24(2):240-56 e9.
58. Clements MP, Byrne E, Camarillo Guerrero LF, Cattin AL, Zakka L, Ashraf A, et al. The Wound Microenvironment Reprograms Schwann Cells to Invasive Mesenchymal-like Cells to Drive Peripheral Nerve Regeneration. *Neuron*. 2017;96(1):98-114 e7.
59. Toma JS, Karamboulas K, Carr MJ, Kolaj A, Yuzwa SA, Mahmud N, et al. Peripheral Nerve Single-Cell Analysis Identifies Mesenchymal Ligands that Promote Axonal Growth. *eNeuro*. 2020;7(3).
60. Hanayama R, Tanaka M, Miwa K, Shinohara A, Iwamatsu A, and Nagata S. Identification of a factor that links apoptotic cells to phagocytes. *Nature*. 2002;417(6885):182-7.
61. Laplante P, Brillant-Marquis F, Brissette MJ, Joannette-Pilon B, Cayrol R, Kokta V, et al. MFG-E8 Reprogramming of Macrophages Promotes Wound Healing by Increased bFGF Production and Fibroblast Functions. *J Invest Dermatol*. 2017;137(9):2005-13.
62. Medzhitov R, and Horng T. Transcriptional control of the inflammatory response. *Nat Rev Immunol*. 2009;9(10):692-703.
63. Gilchrist M, Thorsson V, Li B, Rust AG, Korb M, Roach JC, et al. Systems biology approaches identify ATF3 as a negative regulator of Toll-like receptor 4. *Nature*. 2006;441(7090):173-8.
64. Gey M, Wanner R, Schilling C, Pedro MT, Sinske D, and Knoll B. Atf3 mutant mice show reduced axon regeneration and impaired regeneration-associated gene induction after peripheral nerve injury. *Open Biol*. 2016;6(8).
65. Gill S, Maus MV, and Porter DL. Chimeric antigen receptor T cell therapy: 25years in the making. *Blood Rev*. 2016;30(3):157-67.
66. Newick K, O'Brien S, Moon E, and Albelda SM. CAR T Cell Therapy for Solid Tumors. *Annu Rev Med*. 2017;68:139-52.

67. Maldini CR, Ellis GI, and Riley JL. CAR T cells for infection, autoimmunity and allotransplantation. *Nat Rev Immunol*. 2018;18(10):605-16.
68. Lee S, Kivimae S, Dolor A, and Szoka FC. Macrophage-based cell therapies: The long and winding road. *J Control Release*. 2016;240:527-40.
69. Perry VH, Brown MC, Lunn ER, Tree P, and Gordon S. Evidence that Very Slow Wallerian Degeneration in C57BL/Ola Mice is an Intrinsic Property of the Peripheral Nerve. *Eur J Neurosci*. 1990;2(9):802-8.
70. Boissonnas A, Louboutin F, Laviron M, Loyher PL, Reboussin E, Barthelemy S, et al. Imaging resident and recruited macrophage contribution to Wallerian degeneration. *J Exp Med*. 2020;217(11).
71. Grace PM, Hutchinson MR, Bishop A, Somogyi AA, Mayrhofer G, and Rolan PE. Adoptive transfer of peripheral immune cells potentiates allodynia in a graded chronic constriction injury model of neuropathic pain. *Brain Behav Immun*. 2011;25(3):503-13.
72. Choi J, Kim HY, Ju EJ, Jung J, Park J, Chung HK, et al. Use of macrophages to deliver therapeutic and imaging contrast agents to tumors. *Biomaterials*. 2012;33(16):4195-203.
73. Zhao Y, Haney MJ, Jin YS, Uvarov O, Vinod N, Lee YZ, et al. GDNF-expressing macrophages restore motor functions at a severe late-stage, and produce long-term neuroprotective effects at an early-stage of Parkinson's disease in transgenic Parkin Q311X(A) mice. *J Control Release*. 2019;315:139-49.
74. Pullen TJ, Sylow L, Sun G, Halestrap AP, Richter EA, and Rutter GA. Overexpression of monocarboxylate transporter-1 (SLC16A1) in mouse pancreatic beta-cells leads to relative hyperinsulinism during exercise. *Diabetes*. 2012;61(7):1719-25.
75. Lazarov-Spiegler O, Solomon AS, Zeev-Brann AB, Hirschberg DL, Lavie V, and Schwartz M. Transplantation of activated macrophages overcomes central nervous system regrowth failure. *FASEB J*. 1996;10(11):1296-302.
76. Brown MC, Perry VH, Lunn ER, Gordon S, and Heumann R. Macrophage dependence of peripheral sensory nerve regeneration: possible involvement of nerve growth factor. *Neuron*. 1991;6(3):359-70.
77. Ip WKE, Hoshi N, Shouval DS, Snapper S, and Medzhitov R. Anti-inflammatory effect of IL-10 mediated by metabolic reprogramming of macrophages. *Science*. 2017;356(6337):513-9.
78. Puleston DJ, Buck MD, Klein Geltink RI, Kyle RL, Caputa G, O'Sullivan D, et al. Polyamines and eIF5A Hypusination Modulate Mitochondrial Respiration and Macrophage Activation. *Cell Metab*. 2019;30(2):352-63 e8.
79. Zhang S, Weinberg S, DeBerge M, Gainullina A, Schipma M, Kinchen JM, et al. Efferocytosis Fuels Requirements of Fatty Acid Oxidation and the Electron Transport Chain to Polarize Macrophages for Tissue Repair. *Cell Metab*. 2019;29(2):443-56 e5.
80. Sanin DE, Matsushita M, Klein Geltink RI, Grzes KM, van Teijlingen Bakker N, Corrado M, et al. Mitochondrial Membrane Potential Regulates Nuclear Gene Expression in Macrophages Exposed to Prostaglandin E2. *Immunity*. 2018;49(6):1021-33 e6.
81. Zhou Y, Yu X, Chen H, Sjoberg S, Roux J, Zhang L, et al. Leptin Deficiency Shifts Mast Cells toward Anti-Inflammatory Actions and Protects Mice from Obesity and Diabetes by Polarizing M2 Macrophages. *Cell Metab*. 2015;22(6):1045-58.
82. Huang SC, Smith AM, Everts B, Colonna M, Pearce EL, Schilling JD, et al. Metabolic Reprogramming Mediated by the mTORC2-IRF4 Signaling Axis Is Essential for Macrophage Alternative Activation. *Immunity*. 2016;45(4):817-30.

83. Morioka S, Perry JSA, Raymond MH, Medina CB, Zhu Y, Zhao L, et al. Efferocytosis induces a novel SLC program to promote glucose uptake and lactate release. *Nature*. 2018;563(7733):714-8.
84. Babetto E, Wong KM, and Beirowski B. A glycolytic shift in Schwann cells supports injured axons. *Nat Neurosci*. 2020;23(10):1215-28.
85. Domenech-Estevez E, Baloui H, Repond C, Rosafio K, Medard JJ, Tricaud N, et al. Distribution of monocarboxylate transporters in the peripheral nervous system suggests putative roles in lactate shuttling and myelination. *J Neurosci*. 2015;35(10):4151-6.
86. Minhas PS, Latif-Hernandez A, McReynolds MR, Durairaj AS, Wang Q, Rubin A, et al. Restoring metabolism of myeloid cells reverses cognitive decline in ageing. *Nature*. 2021.
87. Krishnan A, Bhavanam S, and Zochodne D. An Intimate Role for Adult Dorsal Root Ganglia Resident Cycling Cells in the Generation of Local Macrophages and Satellite Glial Cells. *J Neuropathol Exp Neurol*. 2018;77(10):929-41.
88. Yu X, Liu H, Hamel KA, Morvan MG, Yu S, Leff J, et al. Dorsal root ganglion macrophages contribute to both the initiation and persistence of neuropathic pain. *Nat Commun*. 2020;11(1):264.
89. Chandran V, Coppola G, Nawabi H, Omura T, Versano R, Huebner EA, et al. A Systems-Level Analysis of the Peripheral Nerve Intrinsic Axonal Growth Program. *Neuron*. 2016;89(5):956-70.
90. Abe N, and Cavalli V. Nerve injury signaling. *Curr Opin Neurobiol*. 2008;18(3):276-83.
91. Zurborg S, Piszczek A, Martinez C, Hublitz P, Al Banchaabouchi M, Moreira P, et al. Generation and characterization of an Advillin-Cre driver mouse line. *Mol Pain*. 2011;7:66.
92. Madisen L, Zwingman TA, Sunkin SM, Oh SW, Zariwala HA, Gu H, et al. A robust and high-throughput Cre reporting and characterization system for the whole mouse brain. *Nat Neurosci*. 2010;13(1):133-40.
93. Pullen TJ, da Silva Xavier G, Kelsey G, and Rutter GA. miR-29a and miR-29b contribute to pancreatic beta-cell-specific silencing of monocarboxylate transporter 1 (Mct1). *Mol Cell Biol*. 2011;31(15):3182-94.
94. Ma CH, Omura T, Cobos EJ, Latremoliere A, Ghasemlou N, Brenner GJ, et al. Accelerating axonal growth promotes motor recovery after peripheral nerve injury in mice. *J Clin Invest*. 2011;121(11):4332-47.
95. Mordes DA, Morrison BM, Ament XH, Cantrell C, Mok J, Eggan P, et al. Absence of Survival and Motor Deficits in 500 Repeat C9ORF72 BAC Mice. *Neuron*. 2020;108(4):775-83 e4.
96. Liu Y, Latremoliere A, Li X, Zhang Z, Chen M, Wang X, et al. Touch and tactile neuropathic pain sensitivity are set by corticospinal projections. *Nature*. 2018;561(7724):547-50.
97. Yang Y, Lane AN, Ricketts CJ, Sourbier C, Wei MH, Shuch B, et al. Metabolic reprogramming for producing energy and reducing power in fumarate hydratase null cells from hereditary leiomyomatosis renal cell carcinoma. *PLoS One*. 2013;8(8):e72179.
98. Mookerjee SA, and Brand MD. Measurement and Analysis of Extracellular Acid Production to Determine Glycolytic Rate. *J Vis Exp*. 2015(106):e53464.

99. Mookerjee SA, Gerencser AA, Nicholls DG, and Brand MD. Quantifying intracellular rates of glycolytic and oxidative ATP production and consumption using extracellular flux measurements. *J Biol Chem*. 2017;292(17):7189-207.
100. Mookerjee SA, Goncalves RLS, Gerencser AA, Nicholls DG, and Brand MD. The contributions of respiration and glycolysis to extracellular acid production. *Biochim Biophys Acta*. 2015;1847(2):171-81.
101. Oh MH, Collins SL, Sun IH, Tam AJ, Patel CH, Arwood ML, et al. mTORC2 Signaling Selectively Regulates the Generation and Function of Tissue-Resident Peritoneal Macrophages. *Cell Rep*. 2017;20(10):2439-54.

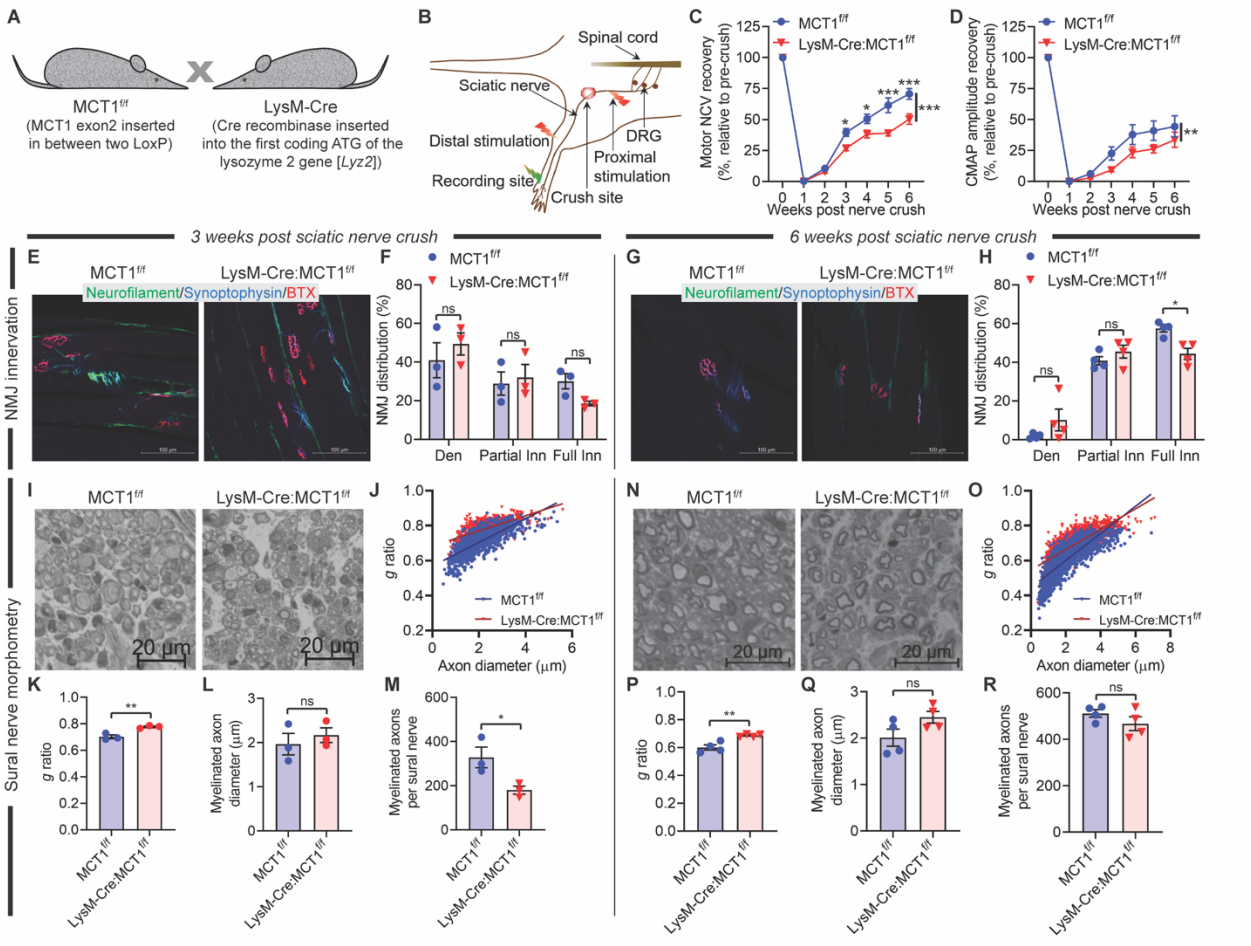

Figure 1. Selective ablation of MCT1 in macrophages impairs axon regeneration. (**A**) MCT1$^{f/f}$ mice were bred with Lysozyme M Cre recombinase mice (LysM-Cre) to generate macrophage-specific MCT1 knockout (LysM-Cre:MCT1$^{f/f}$) and littermate control (MCT1$^{f/f}$) mice. (**B**) Schematic representation of sciatic nerve crush site and electrode setups for electrophysiological studies; DRG, dorsal root ganglion. (**C**) Motor nerve conduction velocity (NCV) and (**D**) compound muscle action potential (CMAP) amplitude recovery of crushed nerve (in percent, relative to pre-crush). Mean ± SEM, n = 13 (for MCT1$^{f/f}$) or 11 (for LysM-Cre:MCT1$^{f/f}$), *P < 0.05, **P < 0.01, ***P < 0.001; vertical line in **C** and **D** represents the overall statistical comparison between the data sets from two genotypes; two-way ANOVA with Bonferroni's multiple comparisons test. Representative photomicrographs of fluorescently

labelled neuromuscular junctions (NMJs) in gastrocnemius muscles (**E** and **G**) after crush. Muscles were stained with α-Bungarotoxin (BTX, red), and antibodies against neurofilaments (SMI312; green) and synaptophysin (blue) to visualize acetylcholine receptors (AChR) and nerve terminals, respectively. Calibration bar: 100 μm. Percentage of fully reinnervated (Full Inn), partially reinnervated (Partial Inn), and denervated (Den) AChR clusters in LysM-Cre:MCT1$^{f/f}$ mice compared with their littermate controls (MCT1$^{f/f}$) 3 (**F**) and 6 weeks (**H**) after crush. Mean ± SEM, n = 3–4 per group, *P < 0 .05; ns = not significant; two-way ANOVA with Bonferroni's multiple comparisons test. (**I** and **N**) Photomicrographs, (**J** and **O**) scatter plot graph displaying g ratio in relation to axon diameter of individual myelinated axons, (**K** and **P**) g ratio, (**L** and **Q**) myelinated axon diameter, and (**M** and **R**) myelinated axon count of sural nerve from LysM-Cre:MCT1$^{f/f}$ and MCT1$^{f/f}$ mice after sciatic nerve crush. Light microscope photomicrographs and subsequent analysis completed on toluidine blue-stained sections. Mean ± SEM, n = 3–4 per group, *P < 0.05; **p <0 .01; ns = not significant, unpaired t test. Calibration bar: 20 μm.

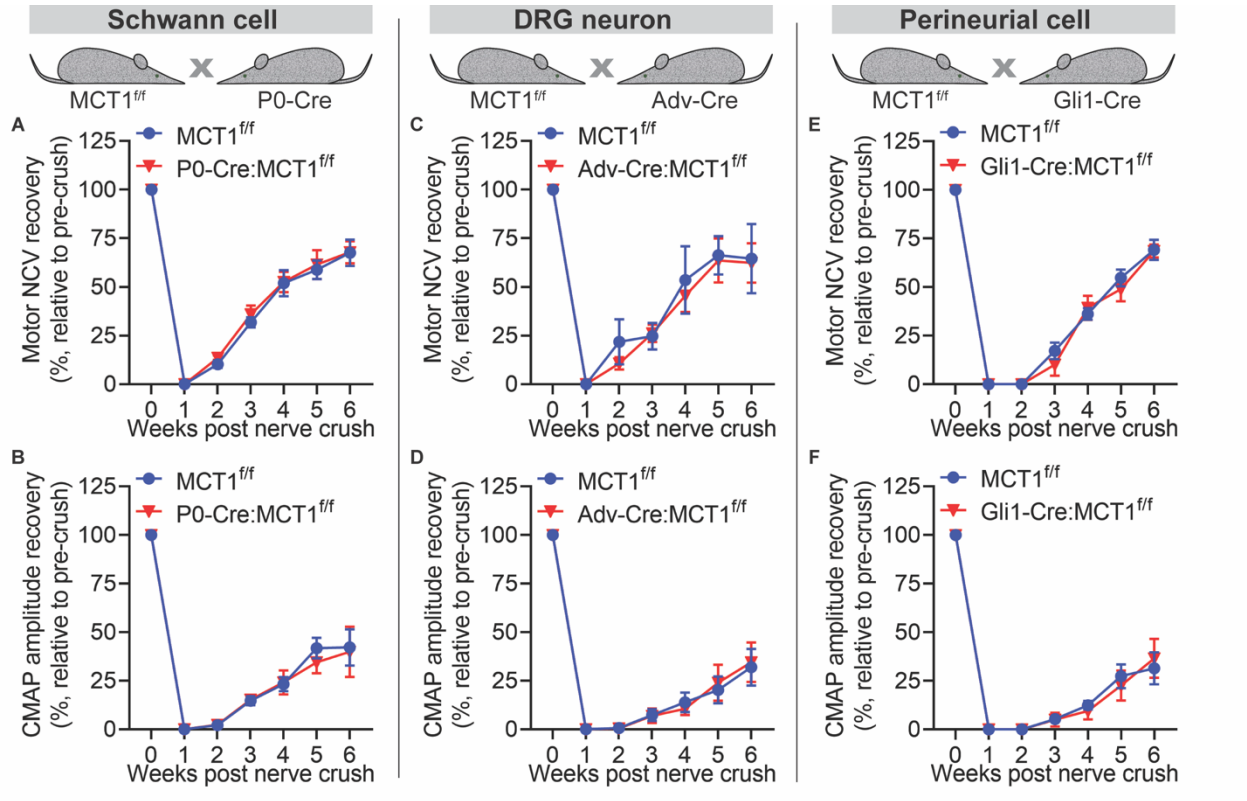

Figure 2. Selective ablation of MCT1 in Schwann cells, DRG neurons, or perineurial cells has no impact on peripheral nerve regeneration. MCT1$^{f/f}$ mice were bred with transgenic mice with Cre recombinase driven by myelin protein zero (P0)-, advillin (Adv)-, or glioma-associated oncogene 1 (Gli1)-Cre to generate Schwann cell, DRG neuron, or perineurial cell-specific MCT1 knockout mice, respectively, and littermate control mice (upper schematic panel). (**A**, **C**, and **E**) Motor nerve conduction velocity (NCV) and (**B**, **D**, and **F**) compound muscle action potential (CMAP) amplitude recovery of nerve was measured after injury. Recoveries are presented as percent relative to pre-crush conditions. No significant difference in NCV or CMAP recovery was found at any time-point due to any cell-specific MCT1 deficiency. Mean ± SEM, *n* = 6 – 10 per group, two-way ANOVA with Bonferroni's multiple comparisons test.

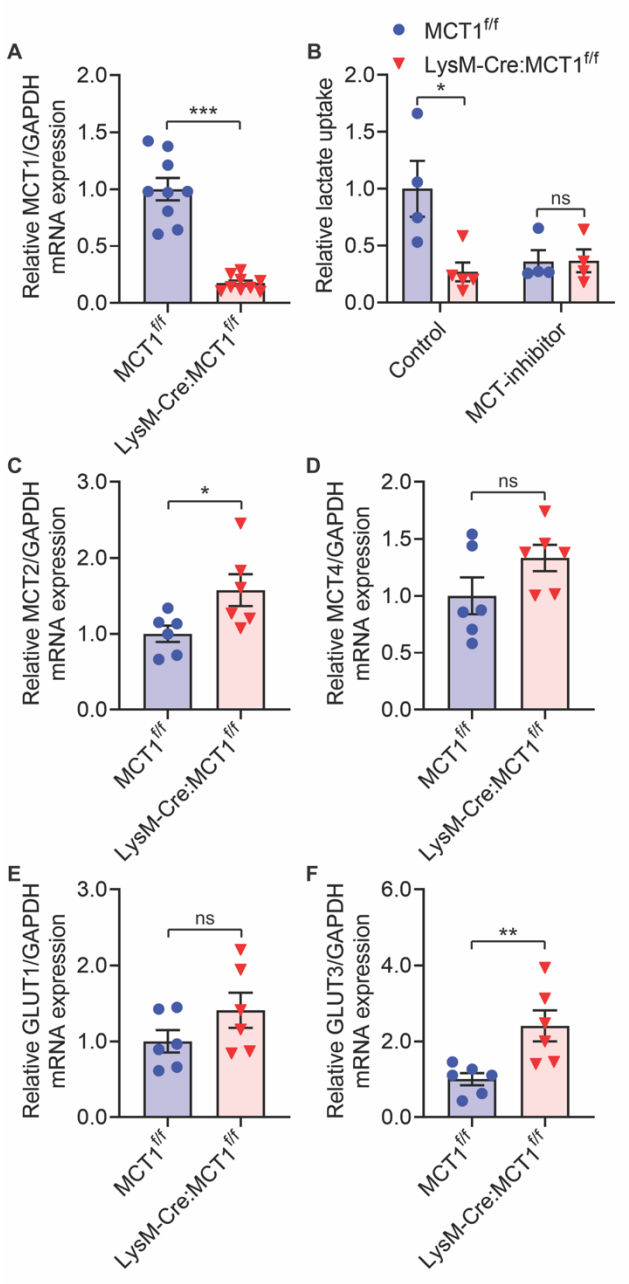

Figure 3. Validation of macrophage-specific MCT1 deficient mice. Expression of monocarboxylate transporters, (**A**) MCT1, (**C**) MCT2, and (**D**) MCT4, and glucose transporters, (**E**) GLUT1 and (**F**) GLUT3, mRNAs was evaluated in peritoneal exudate macrophage cultures prepared from LysM-Cre:MCT1$^{f/f}$ and littermate control (MCT1$^{f/f}$) mice. Levels of mRNAs are depicted as fold change compared with littermate control mice normalized to their corresponding

GAPDH mRNA levels. Mean ± SEM, n = 5–9 per group, *P < 0 .05, **P < 0.01 ***P < 0.001; ns = not significant; unpaired t test. (**B**) Lactate uptake and blockade by selective MCT1 inhibitor in peritoneal exudate macrophage cultures prepared from LysM-Cre:MCT1$^{f/f}$ MCT1$^{f/f}$ mice. Lactate uptake is depicted as fold change relative to MCT1$^{f/f}$ mice. Mean ± SEM, n = 4–5 per group, *P < 0 .05; ns = not significant; two-way ANOVA with Bonferroni's multiple comparisons test.

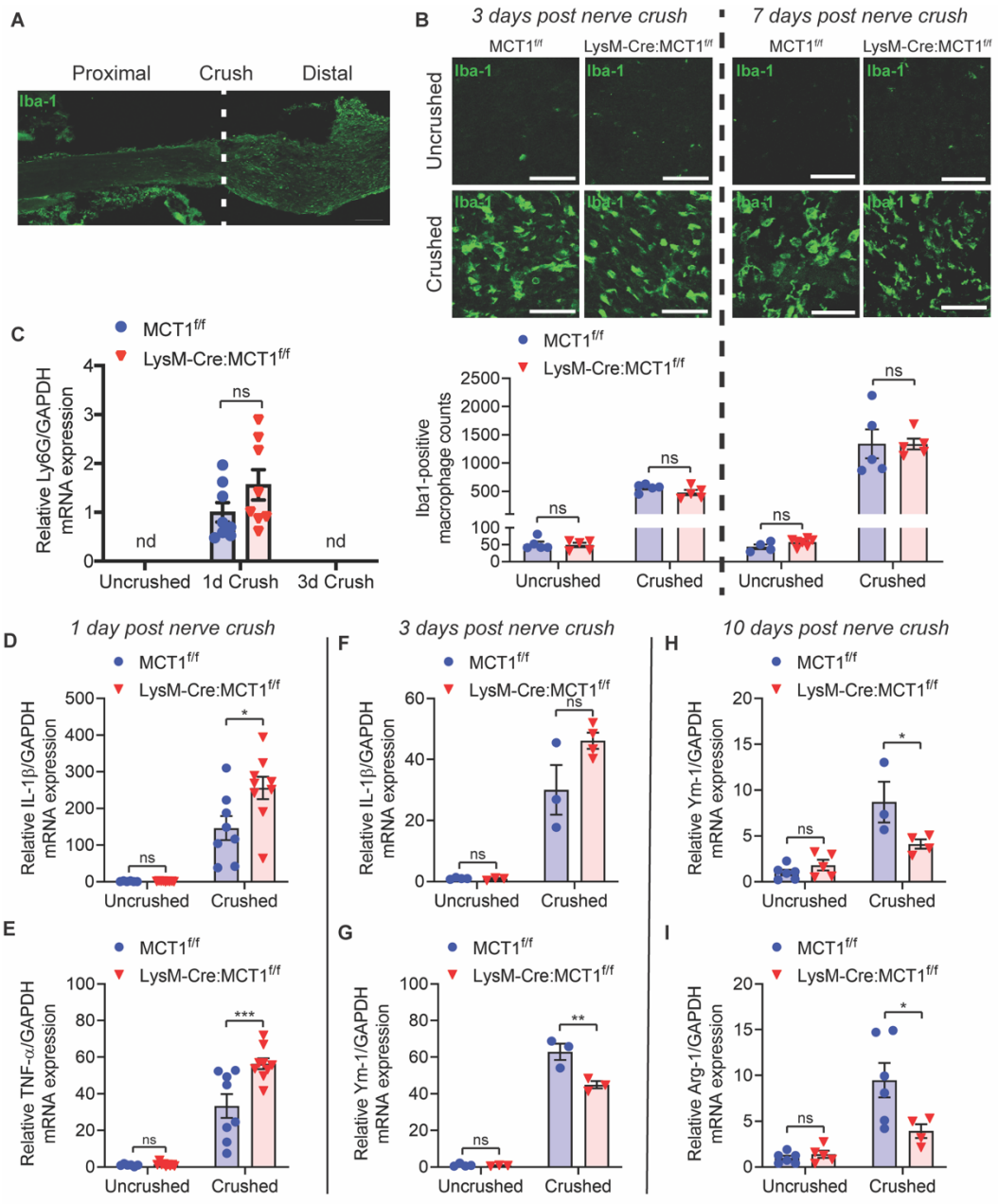

Figure 4. MCT1 ablation in macrophages does not affect the infiltration of Iba1-positive cells but critically modulates inflammatory cytokine expression in injured sciatic nerves. At 3 days (**A** and **B**, left panel) and 7 days (**B**, right panel) post-crush, the number of Iba1-positive macrophages infiltrating into nerves (**B**; representative images from at least four independent experiments) of mice of both genotypes were unchanged (**B**). Total Iba1-positive macrophage

counts were obtained from Z-stack of images of 20 μm thick complete cross-sections of nerve. Mean ± SEM, n = 4–7 per group, ns = not significant, two-way ANOVA with Bonferroni's multiple comparisons test. Calibration bars: 200 μm (**A**) and 50 μm (**B**). (**C**) No change in Ly6G expression in LysM-Cre:MCT1$^{f/f}$ compared to littermate control (MCT1$^{f/f}$) mice, as shown by mRNA expression of Ly6G in uncrushed and crushed sciatic nerves (distal to site of injury) evaluated by real-time RT-PCR. Levels of mRNA are depicted as fold change compared with crushed sciatic nerve (1 day post crush) isolated from MCT1$^{f/f}$ mice normalized to their corresponding GAPDH mRNA levels. Mean ± SEM, nd, not detected; n = 5–8 per group, ns = not significant, unpaired t test. The mRNA expression of IL-1β (**D**) and TNF-α (**E**) at 1 day post crush, IL-1β (**F**) and Ym-1 (**G**) at 3 days post crush, and Ym-1 (**H**) and Arg-1 (**I**) at 10 days post crush in uncrushed and crushed sciatic nerves (distal to site of injury) was evaluated by real-time RT-PCR. Levels of mRNAs are depicted as fold change compared with uncrushed sciatic nerve isolated from MCT1$^{f/f}$ mice normalized to their corresponding GAPDH mRNA levels. Mean ± SEM, n = 3–9 per group, *P < 0 .05; **P < 0.01; ***P < 0.001; ns = not significant, two-way ANOVA with Bonferroni's multiple comparisons test.

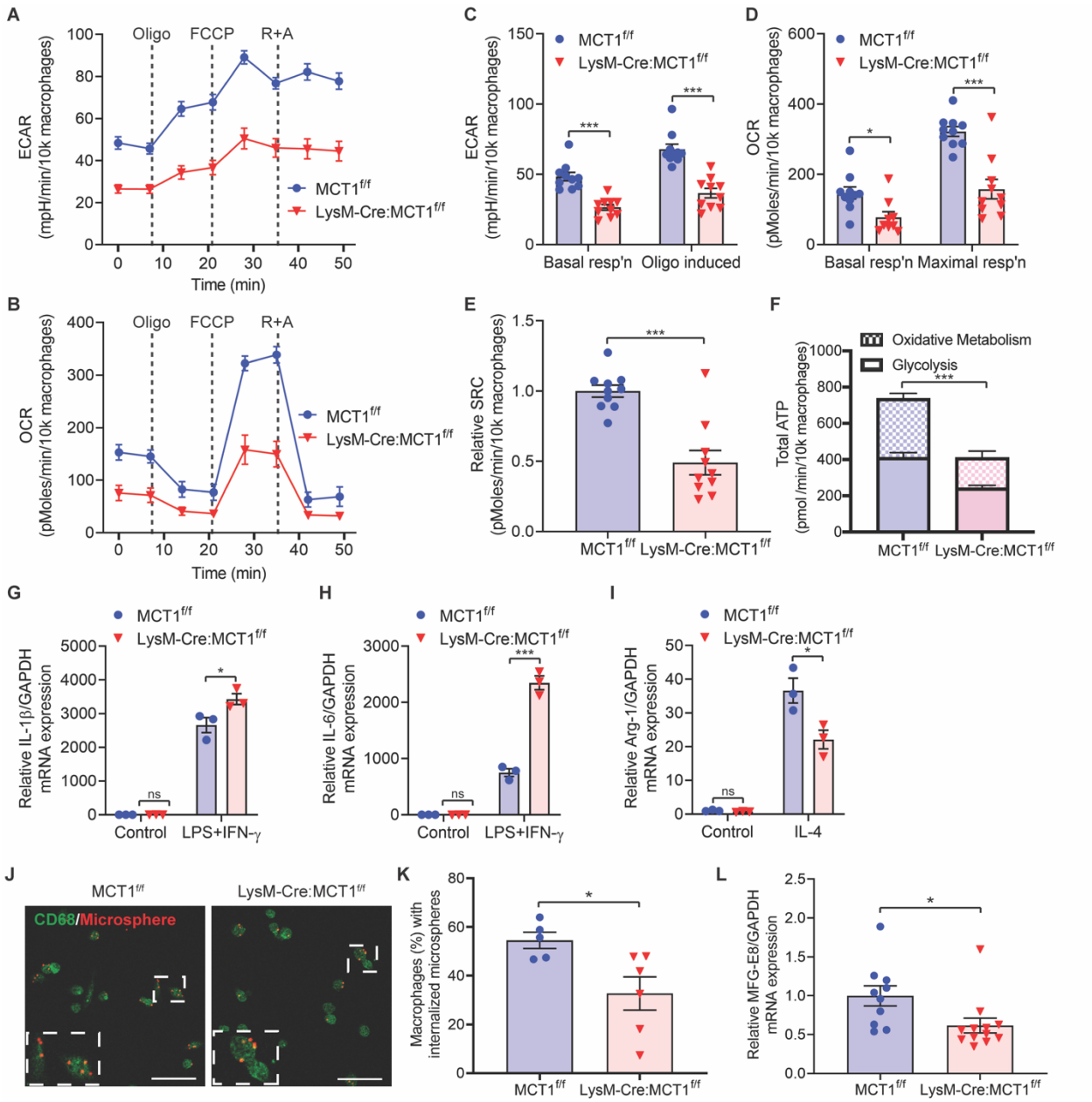

Figure 5. MCT1 ablation impairs metabolic functions, alters expression of inflammatory cytokines, and worsens phagocytic activity of macrophages *in vitro*. Extracellular acidification rate (ECAR, **A**) and oxygen consumption rate (OCR, **B**) were measured in peritoneal exudate macrophages isolated from LysM-Cre:MCT1$^{f/f}$ and MCT1$^{f/f}$ mice with the Seahorse extracellular flux analyzer. (**C**) ECAR was compared during basal conditions and

following oligomycin treatment. (**D**) OCR was compared during basal respiration and FCCP-induced maximal respiration. (**E**) Spare respiratory capacity (SRC, maximal minus basal respiration) was calculated. (**F**) Total ATP generated by oxidative metabolism and glycolysis was calculated. Mean ± *SEM*, $n = 10$ per group, $^{**}P < 0.01$; $^{***}P < 0.001$; two-way ANOVA with Bonferroni's multiple comparisons test for (**C**) and (**D**); unpaired *t* test for (**E** and **F**). FCCP, carbonyl cyanide-4 (trifluoromethoxy) phenylhydrazone; Oligo, oligomycin; R+A; Rotenone and Antimycin. (**G** and **H**) Peritoneal exudate macrophages were treated with LPS (100 ng/ml) plus IFN-γ (50 U/ml) or IL-4 for 3 hours and IL-1β (**G**) and IL-6 (**H**) mRNAs or Arg-1 mRNA (**I**), respectively, were assessed by real-time RT-PCR (fold change relative to littermate control). Mean ± SEM, $n = 3$ per group, $^{*}P < 0.05$; $^{***}P < 0.001$; ns = not significant, two-way ANOVA with Bonferroni's multiple comparisons test. Peritoneal exudate macrophages (30,000 cells/well for the 8-well chamber slide) were incubated with fluorescent microspheres (red) for 2 hours, visualized by immunostaining with anti-CD68 antibody (green), and were imaged by confocal microscopy (**J**; representative images) to determine internalization (percentage of cells with internalized fluorescent microspheres) (**K**). Mean ± SEM, $n = 5–7$ per group, $^{*}P < 0.05$; unpaired *t* test; inset, high magnification image of region marked. Calibration bar: 50 μm. (**L**) Expression of milk fat globule factor-E8 (MGF-E8) mRNA was assessed in peritoneal exudate macrophages (fold change relative to littermate control). Mean ± SEM, $n = 10–12$ per group, ns = not significant; unpaired t test.

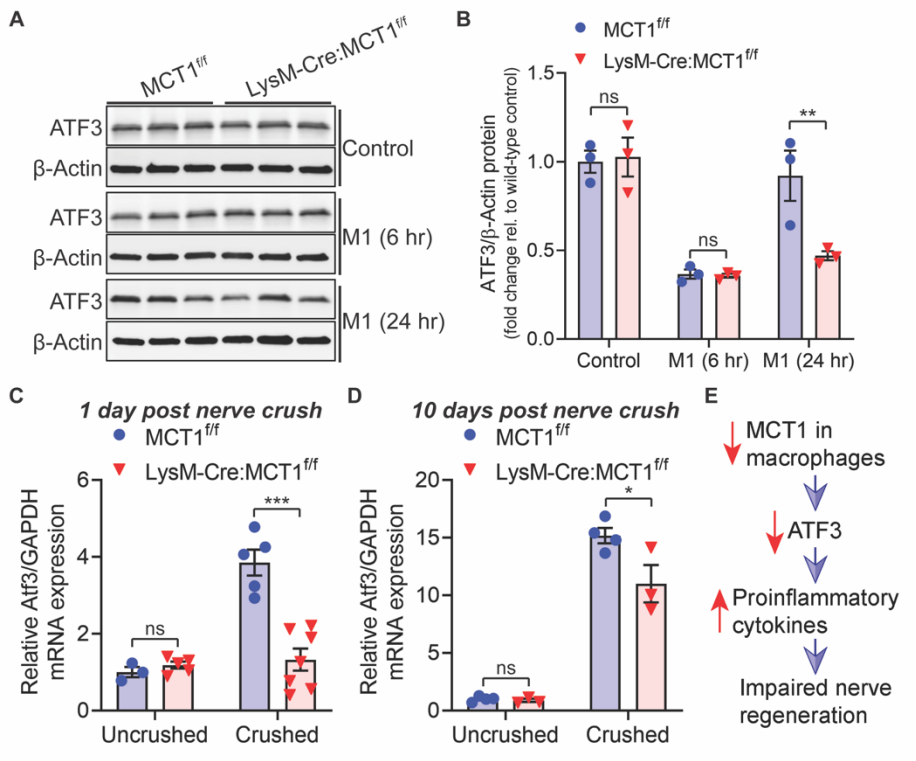

Figure 6. MCT1 determines the immune responses of macrophages potentially though activating transcription factor 3 (ATF3). Peritoneal exudate macrophage cultures prepared from LysM-Cre:MCT1$^{f/f}$ and littermate control (MCT1$^{f/f}$) mice were treated with M1-phenotype inducer mixture [LPS (100 ng/ml) plus IFN-γ (50 U/ml)] for 6 and 24 h. Protein level of ATF3 was assessed by Western blot analysis (**A**). The full-length Western blots were used for the densitometry quantification, and ATF3 expression normalized to β-actin is presented as fold change relative to untreated macrophages from MCT1$^{f/f}$ mice (**B**). Mean ± SEM, $n = 3$ per group, $^{**}p < 0.01$; ns = not significant, two-way ANOVA with Bonferroni's multiple comparisons test. The mRNA expression of *Atf3* at 1 day (**C**) and 10 days (**D**) post injury in uncrushed and crushed sciatic nerves (distal to site of injury) was evaluated by real-time RT-PCR. Levels of mRNAs are depicted as fold change compared with uncrushed sciatic nerve isolated from MCT1$^{f/f}$ mice normalized to their corresponding GAPDH mRNA levels. Mean ± SEM, $n = 3$–7 per group,

*p <0 .05; ***p < 0.001; ns = not significant, two-way ANOVA with Bonferroni's multiple comparisons test. (**E**) Schematic representation of the potential role of MCT1 in nerve regeneration after injury, suggesting that MCT1 deletion in macrophages decreases the expression of ATF3, which leads to increases in expression of proinflammatory cytokines and impaired nerve regeneration.

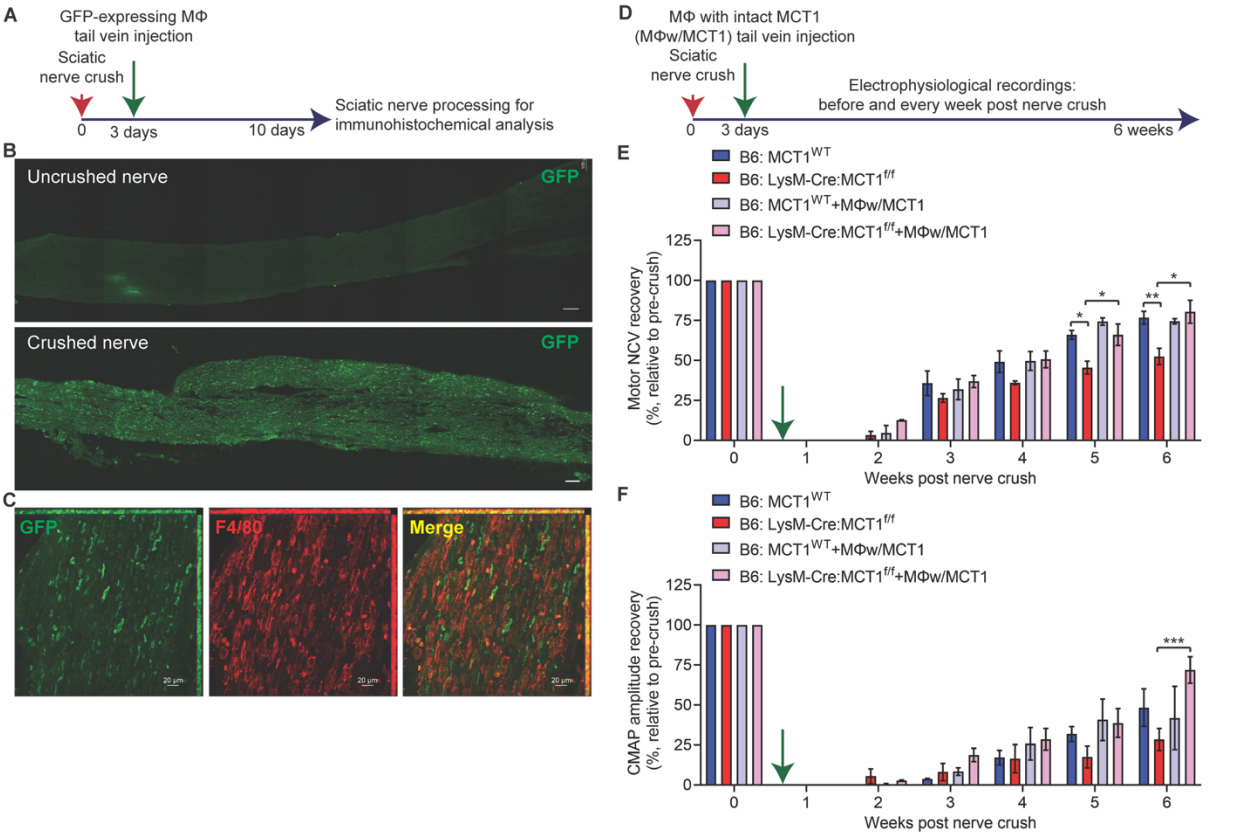

Figure 7. Adoptive cell transfer of macrophages with intact MCT1 ameliorates delayed nerve regeneration in macrophage-specific MCT1 deficient mice. (**A**) Schematic showing intravenous (tail vein) injection of bone marrow-derived macrophages (BMDMs) genetically manipulated to express GFP at 3 days post sciatic nerve crush and processing of the nerves for immunohistochemical analysis at 7 days after injection. Both donors and recipients of same background (C57BL/6J) were used in these studies. BMDMs target the injured (**B**, lower panel), but not the uninjured (**B**, upper panel) sciatic nerve following the intravenous injection. (**C**) High magnification images of nerve samples harvested 7 days following tail vein injection showed that many of the GFP-positive cells (left panel) express F4/80 (red; middle panel), a specific macrophage marker, as can be seen in merged image (right panel). Images are representative confocal micrographs of three independent experiments. Calibration bar: 20 µm. (**D**) Schematic

showing intravenous (tail vein) injection of BMDMs from wild-type mice with intact MCT1 (MΦw/MCT1) at 3 days post sciatic nerve crush and quantification of nerve regeneration by electrophysiology over 6 weeks in C57Bl6 macrophage-selective MCT1 null (B6: LysM-Cre:$MCT^{f/f}$) and wild-type (B6: $MCT1^{WT}$) mice. Both donors and recipients of same background (C57BL/6J) were used in these studies. (**E**) Motor nerve conduction velocity (NCV) and (**F**) compound muscle action potential (CMAP) amplitude recovery of nerve after injury in the following groups: B6: $MCT1^{WT}$, B6: LysM-Cre:$MCT1^{f/f}$, B6: $MCT1^{WT}$ mice following tail-vein injection of BMDMs isolated from B6: $MCT1^{WT}$ mice (B6: $MCT1^{WT}$+ MΦw/MCT1), and B6: LysM-Cre:$MCT1^{f/f}$ mice following tail-vein injection of BMDMs isolated from $MCT1^{WT}$ mice (B6: LysM-Cre:$MCT1^{f/f}$ + MΦw/MCT1). Recoveries are presented as percent relative to pre-crush conditions. Mean ± SEM, $n = 4$ per group, $*P < 0.05$, $**P < 0.01$, $***P < 0.001$; two-way ANOVA with Bonferroni's multiple comparisons test

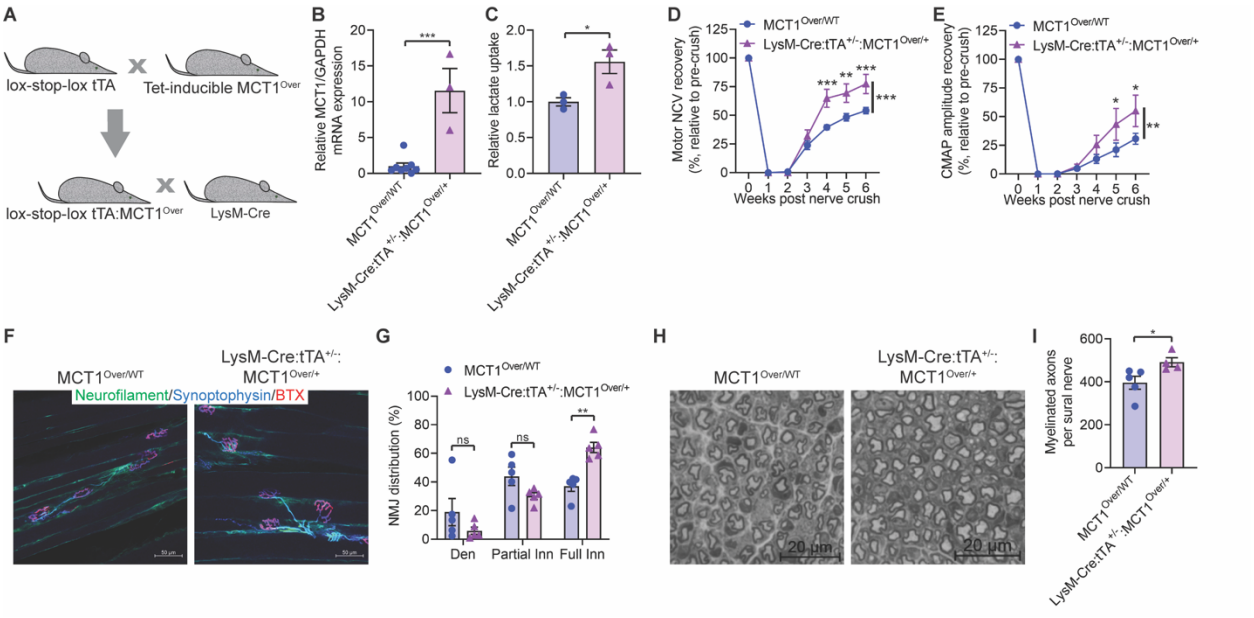

Figure 8. Tet-inducible selective overexpression of MCT1 in macrophages promotes regeneration of injured peripheral nerves. (**A**) Transgenic mice with upregulation of MCT1 selectively in macrophages (LysM-Cre:tTA$^{+/-}$:MCT1$^{Over/+}$) were produced by crossing LysM-Cre mice with lox-stop-lox tTA mice (tet off) and a tet-responsive MCT1 overexpressor mouse. (**B**) MCT1 overexpression was confirmed by evaluating MCT1 mRNA expression in peritoneal exudate macrophages by real-time RT-PCR (fold change relative to littermate control [MCT1$^{Over/WT}$]). Mean ± SEM, n = 3–8 per group, ***$P < 0.001$; unpaired t test. (**C**) Lactate uptake in peritoneal exudate macrophages was assessed and depicted as fold change relative to MCT1$^{Over/WT}$. Mean ± SEM, n = 3 per group, *$P < 0.05$; unpaired t test. (**D**) Motor nerve conduction velocity (NCV) and (**E**) compound muscle action potential (CMAP) amplitude recoveries (in percent, relative to pre-crush) of nerve after injury. Mean ± SEM, n = 8 (for MCT1$^{Over/WT}$) or 6 (for LysM-Cre:tTA$^{+/-}$:MCT1$^{Over/WT}$), *$P < 0.05$, **$P < 0.01$, ***$P < 0.001$; vertical line in **D** and **E** represents the overall statistical comparison between the data sets from two genotypes; two-way ANOVA with Bonferroni's multiple comparisons test. (**F**)

Representative photomicrographs of fluorescently labelled neuromuscular junctions (NMJs) in gastrocnemius muscles 6 weeks after crush. Muscles were stained with α-Bungarotoxin (BTX, red), and antibodies against neurofilaments (SMI312; green), and synaptophysin (blue) to visualize acetylcholine receptors (AChRs) and nerve terminals, respectively. Calibration bar: 50 μm. (**G**) Fully reinnervated (Full Inn), partially reinnervated (Partial Inn), and denervated (Den) AChR clusters 6 weeks after crush. Mean ± SEM, $n = 5$ per group, $^{**}P < 0.01$; ns = not significant; two-way ANOVA with Bonferroni's multiple comparisons test. (**H**) Representative photomicrographs and (**I**) myelinated axon count of sural nerve from LysM-Cre:tTA$^{+/-}$:MCT1$^{Over/+}$ and MCT1$^{Over/WT}$ mice 6 weeks after sciatic nerve crush. Light microscope photomicrographs and subsequent analysis completed on toluidine blue-stained sections. Mean ± SEM, $n = 4–5$ per group, $^{*}P < 0.05$; unpaired *t* test. Calibration bar: 20 μm.